NATIONAL ADVISORY COMMITTEE FOR AERONAUTICS

TECHNICAL NOTE 2339

TRANSONIC FLOW PAST A WEDGE PROFILE WITH DETACHED BOW WAVE - GENERAL ANALYTICAL METHOD AND FINAL CALCULATED RESULTS

By Walter G. Vincenti and Cleo B. Wagoner

Ames Aeronautical Laboratory
Moffett Field, Calif.

Washington
April 1951

NATIONAL ADVISORY COMMITTEE FOR AERONAUTICS

TECHNICAL NOTE 2339

TRANSONIC FLOW PAST A WEDGE PROFILE WITH DETACHED BOW WAVE - GENERAL ANALYTICAL METHOD AND FINAL CALCULATED RESULTS

By Walter G. Vincenti and Cleo B. Wagoner

SUMMARY

Calculations have been made of the aerodynamic characteristics at zero angle of attack of a thin, doubly symmetrical, double-wedge profile for the range of supersonic flight speeds in which the bow wave is detached. The mixed flow over the front half of the profile is determined by a relaxation solution of the transonic small-disturbance equation (the Tricomi equation) in the hodograph plane. The purely supersonic flow over the rear half is found by means of the method of characteristics. No special assumptions are involved in the analysis beyond those implicit in the original differential equation. Calculations for four values of the transonic similarity parameter were found sufficient to bridge the gap between the previous results of Guderley and Yoshihara at a Mach number of 1 and the results which are readily obtained when the bow wave is attached and the flow is completely supersonic.

The results of the study provide the following information as a function of the transonic similarity parameter: (1) shape and location of bow wave and sonic line, (2) chordwise distribution of Mach number and pressure, and (3) integrated pressure drag of front wedge, rear wedge, and complete profile. The important features of these results are noted and discussed. The drag results are also used to illustrate the quantitative indeterminacy which is encountered when the transonic small-disturbance theory is used to obtain results for airfoils of finite thickness at Mach numbers a finite distance from 1.

The present report contains a nonmathematical outline of the theoretical problem and a discussion of the final results. The details of the computations will be covered in a later paper.

INTRODUCTION

At supersonic flight speeds, the flow field about a wedge of infinite span is characterized at zero angle of attack by a symmetrical, two-dimensional shock wave. This wave, which forms either on or in front of the apex of the wedge, is called the bow wave in recognition of its analogy to the surface wave which forms at the bow of a moving

ship. As is well known, the shape of the bow wave and the nature of the flow about the wedge vary depending upon the apex angle of the wedge and the Mach number of the free stream. Consider, for simplicity, the case of a wedge of fixed angle. It will be assumed that the wedge is perfectly sharp and that the effects of viscosity are negligible. It will also be assumed that the wedge is of finite length in the streamwise direction. Under these circumstances, three essentially different regimes of flow are possible, depending upon the Mach number of the free stream:

1. Attached bow wave with purely supersonic flow. – Above a certain free-stream Mach number, the value of which depends upon the magnitude of the wedge angle, the bow wave is attached to the apex of the wedge, and the local flow at all points downstream of the wave is supersonic. Under these conditions, the velocity at the surface of the wedge is uniform, and the bow wave is straight out to its point of intersection with the first Mach wave from the downstream end of the wedge. This regime of purely supersonic flow was first studied by Prandtl and Meyer as long ago as 1908 (reference 1) and is now to be found analyzed in any standard text on gas dynamics.

2. Attached bow wave with mixed subsonic and supersonic flow. – As the free-stream Mach number is reduced in the purely supersonic regime, a condition is eventually reached at which the local velocity downstream of the straight portion of the bow wave is exactly sonic. With further reduction in Mach number, the flow in the vicinity of the wedge becomes subsonic, and the entire fundamental nature of the flow field is altered. For a small range of free-stream Mach number, the bow wave remains attached to the apex but the velocity along the surface of the wedge is now nonuniform. The wave itself, though still inclined toward the rear at all points, is now curved starting from its beginning at the apex. The rather complex sequence of events in this particular regime of mixed subsonic and supersonic flow has been clarified by Guderley (reference 2), but no specific calculations have been made. Since the regime prevails over only a narrow range of Mach number, the lack of quantitative information is not of serious consequence.

3. Detached bow wave. – At a free-stream Mach number slightly below that which gives sonic flow behind the bow wave, a limiting condition is reached below which an attached wave is no longer possible. At lower Mach numbers, therefore, the wave detaches from the apex and stands in the stream forward of the wedge. In this regime of flow, which prevails down to a Mach number of unity, the subsonic flow over the surface of the wedge has a stagnation point at the apex. The element of the curved bow wave directly ahead of the apex is now normal to the direction of the free stream. This regime of mixed flow may occupy a considerable interval of Mach number in the currently

important range of transonic flight speeds. Because of difficulties inherent in the mathematics of the problem, however, quantitative theoretical results free of special assumptions are generally lacking.

Perhaps the first calculations of the flow about a finite wedge with a detached bow wave were made by Maccoll and Codd in England between 1938 and 1942 (reference 3) and were reported by Maccoll at the 6th International Congress of Applied Mechanics in Paris in 1946 (reference 4). In this initial work, the computations were carried out in the plane of physical coordinates – or, more precisely, in a plane of distorted physical coordinates. For reasons which will appear later, a direct solution was not possible with this approach, so that recourse was had to a method of successive approximations. The successive approximations were obtained by numerical integration of the partial differential equations of fluid motion in the subsonic portion of the flow field. By this means Maccoll and Codd were able to obtain results for the mixed flow about bodies of various shape. The calculations for the wedge with a detached wave were confined, however, to the single case of a free-stream Mach number of 1.5 and a total wedge angle of 40°.

An alternative method of analysis, which eliminates the need for successive approximations, has been described independently by Frankl (1945) in Russia and by Guderley (1947) in this country (references 5 and 2, respectively). In this approach, the problem of the wedge with a detached wave is formulated as a boundary-value problem with the velocity components as the independent variables. Using this hodograph method, Frankl was able to prove that the solution of the detached-wave problem is unique. (This had been tacitly assumed by Maccoll and Codd.) Guderley, following a similar approach, showed how the hodograph problem can be simplified by restriction to small disturbances about the sonic velocity. These developments have been subsequently reviewed in non-mathematical form by Busemann (reference 6). More recently (1949), Guderley and Yoshihara, using the small-disturbance theory, have obtained a quantitative solution for the finite wedge at a free-stream Mach number of unity (reference 7). In this special limiting case, the bow wave disappears at infinity upstream, which facilitates the mathematical analysis. The corresponding boundary-value problem in the hodograph plane was solved analytically by Guderley and Yoshihara with the aid of Fourier analysis and a harmonic analyzer. For free-stream Mach numbers greater than unity, a comparable analytical solution of the boundary-value problem is not yet available. Such a solution would appear, indeed, to present serious mathematical difficulties, even in the relatively simple small-disturbance theory.[1]

[1]The references cited in the foregoing discussion approach the solution of the finite-wedge problem through wholly theoretical analysis of the details of the flow phenomena in the complete flow field. Papers which deal with other problems involving detached shock waves or with other approaches applicable to the finite-wedge problem are listed for the convenience of the interested reader in a bibliography at the end of the report.

The work to be described in the present report is a logical extension and application of the hodograph method of Guderley and Frankl. To circumvent the lack of an analytical solution at Mach numbers greater than 1, it was proposed in the present study to solve the boundary-value problem by means of numerical techniques. In the application of numerical methods, the present work has much in common with the investigations of Maccoll and Codd. The use of the hodograph approach, however, eliminates the need for successive approximations and brings about other improvements in ease and rigor. Furthermore, through use of the similarity principles inherent in the small-disturbance theory, general results applicable to any thin wedge can be obtained on the basis of a relatively small number of specific calculations. In the present work, these results are used, in particular, to study the pressure distribution and drag of a complete, doubly symmetrical double-wedge profile in the range of flight Mach numbers from unity upwards.

While the present theoretical investigation was in progress, information was received that a parallel experimental study of the flow over a finite wedge had been undertaken by Hans W. Liepmann and Arthur E. Bryson, Jr., at the California Institute of Technology. Although the two investigations were planned quite independently, the direct relationship of their subject matter makes it desirable that they be reported in related fashion. It has been decided, therefore, to present the detailed results of both studies in a series of three coordinated papers to be published by the NACA under a common general title. The present report, which is the first of this series, contains a largely nonmathematical outline of the theoretical problem and a discussion of the final calculated results. The lengthy details of the computations will be dealt with in a second report by the present authors. The third report, to be written by Bryson, will contain a description of the experimental investigation carried out at the California Institute of Technology and a comparison of the theoretical and experimental results. Certain of the results which will appear in these reports have been given in preliminary form by Liepmann and Bryson in reference 8.

NOTATION

Primary Symbols

a_* critical velocity (i.e., velocity at which the velocity of flow and the velocity of sound are equal)

c airfoil chord

c_d drag coefficient

$\tilde{c}_d$ generalized drag coefficient (See equation (11).)

C_p	pressure coefficient
$\tilde{C}_p$	generalized pressure coefficient (See equation (8).)
$f(x/c)$	function defining shape of profile
M	Mach number
p	static pressure
q	dynamic pressure $\left(\frac{\gamma}{2} p M^2\right)$
t/c	airfoil thickness ratio
u	horizontal component of velocity
v	vertical component of velocity
x,y	Cartesian coordinates
$\tilde{Y}$	ordinate function (See equation (2).)
γ	ratio of specific heats (1.4 for air)
θ	stream inclination
ξ	speed function (See equations (4) and (20).)
ξ_o	transonic similarity parameter (See equations (1) and (21).)

Subscripts

o	conditions in free stream
$*$	conditions at sonic point on airfoil
f	front portion of airfoil
r	rear portion of airfoil
$M_o=1$	value at free-stream Mach number of 1
$\xi_o=0$	value at $\xi_o=0$

GENERAL THEORETICAL METHOD

Description of Flow Field

It is convenient to begin by examining the nature of the flow field which exists around a doubly symmetrical, double-wedge profile when the bow wave is detached. The complete double-wedge profile is considered here since the determination of the characteristics of this profile is the final object of the present work. The description and results relative to the flow over the forward half of this profile, however, are applicable, within minor limitations, to the flow over any finite wedge which terminates in a sharp convex corner. It will be assumed in all that follows that the fluid surrounding the profile is a perfect gas and that the effects of viscosity and thermal conductivity are negligible.

Under these idealized conditions, the flow about a nonlifting double-wedge profile with a detached bow wave is qualitatively as shown in the accompanying sketch. (Since the flow is symmetrical about the chord line, only the upper half of the field is shown.) As indicated,

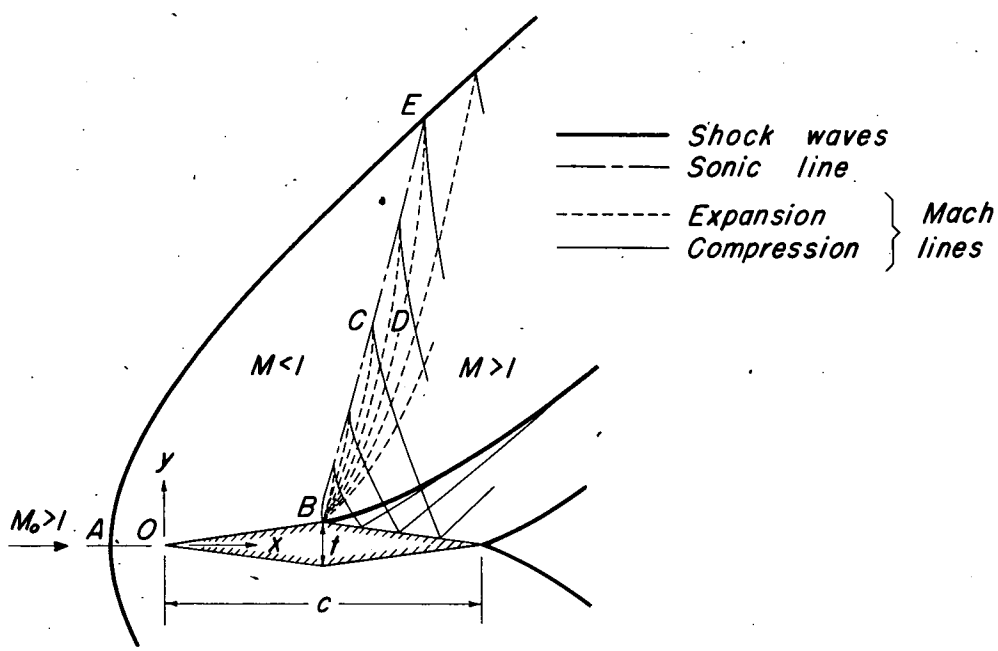

the subsonic flow which exists behind the detached wave is confined to a limited region bounded by the wave, the sonic line, and the forward half of the profile. The fluid which enters this region is decelerated discontinuously from supersonic to subsonic velocity in passing through the detached shock wave. Downstream of the shock wave, the fluid is accelerated continuously, first to the speed of sound at the sonic line and then to supersonic speed beyond this line. As previously mentioned, the detached bow wave begins normal to the free stream at the axis of symmetry (point A) and curves progressively downstream. Far from the airfoil, the slope of the wave tends asymptotically to the slope of a free-stream Mach line. Since the detached wave is curved, the flow behind the wave is, of course, nonuniform. The sonic line, which forms the downstream boundary of the subsonic region, begins at the ridge of the profile (point B) and extends to some point E on the shock wave. Since the flow in the subsonic region is nonuniform, the sonic line is curved. As can be demonstrated, however, it must leave the ridge normal to the forward surface of the profile.

Directly to the rear of the sonic line at the ridge, a supersonic expansion fan originates. This expansion fan tends, in the immediate vicinity of the ridge, toward a simple Prandtl-Meyer flow, in which the sonic line and the elementary Mach waves would be straight lines emanating radially from the corner. Since the sonic line in the present flow is curved, however, the Mach waves of the expansion fan must be curved as well, the curvature being in the forward direction. By virtue of this forward curvature, certain of the expansion waves meet the sonic line, while others meet the outer portion of the bow wave. One particular expansion wave BDE meets both the sonic line and the bow wave at their common point E. This particular wave may be termed the "separating wave," since it separates the expansion waves into two classes: those which reach the sonic line and those which do not. It is apparent that any small disturbance introduced into the expansion fan forward of the separating wave BDE will travel along a Mach wave to a point on the sonic line. From there it will spread throughout the subsonic region, thereby influencing the shape of the sonic line and, hence, of the expansion fan itself. The entire subsonic region and the limited portion BDECB of the adjacent supersonic region are thus interdependent and must be regarded for analytical purposes as a single, bounded transonic zone. A small disturbance originating in the purely supersonic region to the rear of the separating wave BDE cannot reach the sonic line and can have no effect upon the flow in the afore-mentioned transonic zone.

The supersonic flow over the rear of the airfoil is directly influenced by conditions in the transonic part of the field. Analysis indicates that the elementary expansion waves which reach the sonic line do not terminate there but are reflected as elementary compression waves. These waves are again reflected as compression waves at the solid surface of the airfoil. After this last reflection, the elementary compression waves coalesce to form an oblique shock wave which begins at

the ridge. On thin sections this shock wave is very weak and may be regarded, for all practical purposes, as a distributed compression. Rearward of the oblique wave from the ridge, the flow continues with supersonic velocity to the trailing edge, where there is a second oblique shock wave of the type familiar from purely supersonic airfoil problems.

Method of Analysis

To handle the present problem analytically, the flow must first be determined in the transonic zone bounded by the bow wave, the airfoil profile, and the separating Mach wave. As in all transonic problems, such determination involves the solution of a partial differential equation of mixed type, that is, one which is elliptic in the subsonic region and hyperbolic in the adjoining supersonic region. The solution of an equation of this type is troublesome at best. In the present problem, however, additional difficulties arise. First of all, the differential equation, beside being of the mixed type, is also nonlinear. Second, the location of two of the boundaries of the transonic zone - the bow wave and the separating Mach wave - is not known a priori but must be determined as part of the solution. Third, the flow in the transonic zone, having passed through the curved bow wave, is necessarily rotational.

The foregoing difficulties seriously complicate any attempt to solve the problem in the physical plane, even when numerical techniques are employed. The nonlinearity of the differential equation, though it does not preclude a solution by numerical methods, does greatly increase the amount of numerical work over that which is ordinarily encountered with a linear equation. The lack of knowledge concerning the location of the boundaries of the transonic zone can be overcome by resorting to a method of successive approximations, as in the work of Maccoll and Codd (references 3 and 4). Such a procedure, however, entails considerably more labor than would be required if the boundaries were known at the outset.[2] The difficulties due to the fluid rotation can be disposed of simply by

[2] Maccoll and Codd simplify both the fundamental problem and the calculative procedure by taking the sonic line, instead of the separating Mach wave, as the downstream limit of the region of calculation. This eliminates the need for considering the mathematical singularity which exists behind the sonic line at the ridge, but requires in return that some condition be specified along the sonic line itself. This requirement is met by assuming that the streamlines and the sonic line are mutually perpendicular and that the sonic line may be represented by a suitable parabola. The error introduced by these special assumptions is not known, but would probably be considerable for thin wedges at low supersonic speeds.

assuming that the rotation is negligible. The inaccuracies introduced by this assumption are undoubtedly small, except for thick wedges moving at relatively high Mach numbers. Even with the rotation eliminated from the equations, however, the basic nonlinearity still remains.

In addition to the theoretical difficulties just discussed, there exists also a practical complication which is important from the computational point of view. This complication arises from the fact that any rigorous solution of the problem must be a function of three independent variables: the free-stream Mach number M_o, the thickness ratio t/c, and the ratio of specific heats γ. Thus, if a rigorous theory is used, a considerable number of cases must be calculated to obtain an adequate cross section of numerical results.

As in the work of Guderley and Frankl (references 2 and 5), the first step in the solution of the problem is to transform the flow from the physical plane to the hodograph plane. This affords an immediate simplification by providing a completely fixed set of boundaries for the transonic zone. The bow wave, in particular, goes over into a known shock polar, while the separating Mach wave transforms into one of the fixed epicycloids which make up the characteristic net in the hodograph. The differential equation in the hodograph variables is still of the mixed type, as would be expected in view of the transonic nature of the original problem. The equation is also still nonlinear if the fluid rotation is included in the analysis. If the rotation is arbitrarily neglected, however, the differential equation in the hodograph becomes linear, in contrast to the previous situation in the physical coordinates.[3] Since the fundamentals of the problem are unchanged by the transformation to the hodograph, the complication still remains that any solution must be a function of the three variables mentioned above.

The second major step in the analysis is to introduce the assumption of small disturbances. Specifically, it is assumed that the entire flow field, including the free stream, differs only slightly from a parallel sonic flow. From the physical point of view, this assumption implies that the results of the theory are restricted to thin airfoils at flight Mach numbers not far removed from 1. From the mathematical point of view, it means that quantities such as t/c and (M_o^2-1) are regarded as arbitrarily small so that only their lowest powers need be retained in the analysis. As is well known, this small-disturbance approximation brings about important simplifications in the mathematics of the problem. First, the terms representing fluid rotation turn out to be of the same order as other terms which are neglected in the analysis. This means that the use of the linear differential equation in the hodograph is

[3]Frankl's uniqueness proof, mentioned in the introduction, is based on the linear equation and thus ignores the fluid rotation. It seems unlikely, however, that the inclusion of rotational effects would alter the conclusions of this study.

strictly justified within the framework of the approximate theory. Second, the differential equation itself, though still of mixed type, takes on an especially simple form (the Tricomi equation). This equation has been the subject of considerable mathematical study, beginning with the work of Tricomi (reference 9). Third, the solution of the problem becomes a function of a single parameter which involves all three of the individual variables previously discussed. This single parameter is known as the transonic similarity parameter and will be denoted here by the symbol ξ_0. It can be written in several forms, as, for example,

$$\xi_0 \cong \frac{M_0^2-1}{[(\gamma+1)\ (t/c)]^{2/3}} \tag{1}$$

The use of this last simplification greatly reduces the amount of computation required to investigate the effects of changes in the individual variables.

It may be remarked in passing that the foregoing assumption of small disturbances will obviously be violated near the stagnation point which exists at the leading edge of the profile. A similar situation is, of course, encountered in the classical theory of thin airfoils at purely subsonic speeds. There the inconsistency is known to be of little practical consequence except in the immediate vicinity of the leading edge itself. It is to be expected that the same result will prevail in the locally subsonic flow encountered here.

As mentioned in the introduction, a detailed account of the formulation and solution of the boundary-value problem in the hodograph plane will be reserved for a later paper. It must suffice here to say that the boundaries and boundary conditions are taken essentially as given by Guderley (reference 2), except that the supersonic portion of the transonic zone is replaced by an equivalent integral relation which must be satisfied everywhere along the sonic line. By this modification, which involves no approximations beyond those already employed, the mathematical problem is reduced to that of solving a purely elliptic differential equation. This was found essential to the numerical solution of the problem. The solution itself is carried out according to methods well established for the numerical treatment of partial differential equations (see, e.g., references 10, 11, and 12). As usual, the domain under consideration is first covered with a graded, square mesh; and a finite-difference approximation of the differential equation or boundary condition is written for each mesh point. By this means the original boundary-value problem for the partial differential equation is reduced to the theoretically simpler problem of finding the solution of a large system of simultaneous algebraic equations. The latter problem is solved in normal fashion by the application of relaxation techniques. The methods employed throughout are standard, except for the use of somewhat

novel procedures in formulating the finite-difference equations along the shock polar and sonic line.[4]

Once the solution for the front half of the airfoil is determined in the hodograph plane, the transformation back to the physical plane is a simple matter. The purely supersonic flow over the rear half is then constructed in the physical plane by means of the method of characteristics as specialized to the small-disturbance theory.

It will be noted that the solution of the problem in the present manner, though laborious because of the use of numerical techniques, requires no special assumptions beyond those implicit in the differential equations. In particular, no restrictions are necessary with regard to the geometric shape of the shock wave or sonic line.

Although the transonic small-disturbance theory was originally formulated for the solution of problems of mixed flow, it is not confined in its applications to problems in which such flow actually occurs. The theory may still be applied - in simple analytical form, in fact - in the completely supersonic regime, where the bow wave is attached and the region of subsonic flow has disappeared. This is accomplished by first reducing the complete equations for the oblique shock wave and the Prandtl-Meyer expansion to appropriate forms involving the transonic similarity parameter (see, for example, the work of Tsien and Baron, reference 13) and then applying these results as in the standard shock-expansion method. This procedure is applicable to the present airfoil when $\xi_0 \geq 2^{1/3} = 1.260$, this being the condition, to the order of accuracy of the small-disturbance theory, for an attached wave with not less than sonic flow on the downstream side.[5] (Consistent with the remarks in the introduction, attachment of the wave itself takes place at the somewhat lower value of $\xi_0 = 3/(4)^{2/3} = 1.191$.)

---

[4] As is often the case with relaxation work, the numerical calculations made considerable demands upon the skill and perseverance of the computer. Special credit is due Mrs. Helen Mendel for the successful completion of this phase of the study.

[5] In the shock-expansion method it is assumed that the pressure is uniform on each straight-line segment of the airfoil surface. Because of interaction effects between the shock wave from the bow and the expansion fan from the ridge, this condition is not completely fulfilled until the flow behind the bow wave is somewhat greater than sonic, that is, until the value of ξ_0 is somewhat above 1.260. In conformity with usual practice, this complication is ignored in the present work since it is known to have only a negligible influence upon the computed characteristics of the airfoil.

RESULTS IN TRANSONIC SIMILARITY FORM

Calculations have been carried out, according to the numerical methods described in the preceding section, for four values of the similarity parameter ξ_0; namely, 0.484, 0.703, 0.921, and 1.058. These four cases were found sufficient to bridge the gap between the findings of Guderley and Yoshihara at $M_0 = 1$ ($\xi_0=0$) and the analytical results which are available when the bow wave is attached and the flow is everywhere supersonic ($\xi_0 \geq 1.260$). The complete results of the calculations will be presented in the present section in transonic similarity form, that is, in the generalized form which arises directly out of the small-disturbance theory. The application of the drag results to a specific airfoil (i.e., to a given value of t/c) will be discussed in a later section of the report.

Bow Wave and Sonic Line

The generalized ordinates of any chosen line which intersects the streamlines are given in the transonic small-disturbance theory by an ordinate function of the form

$$\tilde{\tilde{Y}} = \tilde{\tilde{Y}}\left(\frac{x}{c}, \xi_0\right) \tag{2}$$

where x/c is the actual abscissa and ξ_0 is the transonic similarity parameter. The actual ordinates y/c for given values of M_0, t/c, and γ can be approximated by means of the relation

$$\tilde{Y} \cong [(\gamma+1)(t/c)]^{1/3}\left(\frac{y}{c}\right) \tag{3}$$

(For derivation of the transonic similarity laws on which these and later equations are based, see references 14, 15, 16, or 17.) The calculated shape of the bow wave and sonic line is shown in figure 1 in terms of the foregoing quantities.

To facilitate the discussion, the results of figure 1 and of the succeeding similarity plots will often be spoken of as if they were directly applicable to fixed values of t/c and γ. Thus, a decrease toward zero in the similarity parameter will sometimes be described simply as a decrease toward 1 in the free-stream Mach number. As will be seen in a later section of the report, this interpretation is necessarily somewhat loose from the quantitative point of view. It does, however, lend a useful physical significance to the similarity plots.

In a figure such as the present one, in particular, an appreciation of physical proportions can be achieved by dividing $\bar{Y}$ by the numerical factor $(0.24)^{1/3}$ and plotting the results to equal vertical and horizontal scales. Thus, for the specific conditions of $t/c = 0.10$ and $\gamma = 1.4$ (air), the vertical scale reads directly in values of y/c, and the figure provides as it stands a geometrically correct representation of the flow field. The corresponding values of M_o, as approximated from equation (1), are given by the upper figure along the shock wave. (On the same basis, the sonic velocity will first appear in the flow field about the 10-percent-thick section at a free-stream Mach number of approximately 1.219 ($\xi_o = 1.260$). Detachment of the shock wave will occur at the slightly lower Mach number of 1.208 ($\xi_o = 1.191$).)

The dashed outline of the airfoil which appears in figure 1 is to be regarded as a diagrammatic representation only. In a similarity plot of this kind, the profile must be regarded, properly speaking, as coinciding with the horizontal axis. (For a more complete discussion of this point see page 29 of reference 18.) The dashed profile in figure 1 is included only as an aid in orienting the reader.

It will be noted that in each case in figure 1 the shock wave and sonic line as calculated do not meet at a common point. This discrepancy appears in the course of the transformation from the hodograph to the physical plane; it is primarily a reflection of the fact that a solution of the system of finite-difference equations in the hodograph is not an exact solution of the boundary-value problem for the original partial differential equation. This so-called "truncation error" can, in principle, be made as small as desired by progressively decreasing the mesh size in the hodograph. In the present work this procedure has been carried in each case to the point where increased refinement caused only an insignificant change in the pressure distribution or over-all drag. Because of the nature of the hodograph transformation, however, the details of the accompanying flow field are subject to somewhat greater error, particularly with regard to the over-all height of the subsonic region. As implied by the size of the gap between the shock wave and sonic line, the absolute magnitude of this error increases as ξ_o decreases, though the percentage error in terms of the height of the subsonic region is nearly constant. The actual magnitude of the truncation error is in all cases certainly less than the errors caused by the basic theoretical assumption of small disturbances.

It is seen in figure 1 that in each case the calculated sonic line begins at the midchord point at right angles to the horizontal axis. This result is consistent, to the accuracy of the small-disturbance theory, with the known fact that the sonic line given by any rigorous treatment would leave the ridge normal to the forward surface of the profile. As it leaves the airfoil, the sonic line curves at first rather sharply toward the rear. The initial curvature can, in fact, be shown to be infinite. A short distance from the airfoil, the

rearward trend is reversed, with the result that the sonic line has a predominately forward curvature over most of its length. The flow across most of the sonic line in the present problem is apparently analogous to the accelerating transonic flow through a continuous-walled, converging-diverging nozzle, where the sonic line is known to have a consistently forward curvature. The rearward curvature which is evident close to the airfoil is only a localized effect caused by the presence of the sharp corner at the ridge.

The rapidity with which the subsonic region expands vertically with reduction in the free-stream Mach number is striking. For the airfoil of 10-percent thickness ratio, for example, the semiheight of the subsonic region in figure 1 grows from approximately 2.4 chord lengths at $M_o \cong 1.187$ to approximately 18.3 chord lengths at $M_o \cong 1.090$. The height of the subsonic region (and the distance of the shock wave ahead of the airfoil) would, of course, tend to infinity as the Mach number approached still closer to unity. These results imply that the tip effects are likely to be considerable on finite-span wings at free-stream Mach numbers close to 1.

According to the transonic similarity laws, the speed of flow at any point in the generalized flow field is determined by the local value of a dimensionless speed function ξ, which can be written in one of its several forms as

$$\xi \cong \frac{M^2-1}{[(\gamma+1)(t/c)]^{2/3}} \tag{4}$$

where M is the local value of the Mach number. (The transonic similarity parameter is thus merely the special value of the speed function which applies at points in the free stream.) As a matter of interest, contours of constant speed function ξ in the region between the shock wave and sonic line have been determined for the case of $\xi_o = 0.921$. These results are shown in figure 2. By virtue of equation (4), the contours of constant ξ may be interpreted, for fixed values of t/c and γ, as contours of constant Mach number. They may also be regarded, to the order of accuracy of the transonic small-disturbance theory, as contours of constant velocity, pressure, density, and temperature. It will be noted that certain of the contours, in common with the sonic line, fail to meet the shock wave. This again is a reflection of errors inherent in the finite-difference solution.

Chordwise Distribution of Mach Number and Pressure

At points on the surface of the airfoil, the speed function ξ is related to the similarity parameter ξ_o by an equation of the form

$$\xi = \xi\left(\frac{x}{c}, \xi_0\right) \tag{5}$$

The calculated values of ξ at the surface of the airfoil are shown in figure 3 for the four values of the similarity parameter. Also included in the figure are results for $\xi_0 = 0$ as obtained from the previously cited work of Guderley and Yoshihara (reference 7). In line with the earlier interpretation, the curves of figure 3 may be looked upon here as representing the chordwise distribution of Mach number for fixed values of t/c and γ but different values of M_0.

All of the distribution curves of figure 3 have the same general shape. In each case, for example, the calculated Mach number at the leading edge has an infinite negative value. This physically impossible result, which is characteristic of small-disturbance theories in general, represents the stagnation condition which must prevail in the real subsonic flow at the leading edge. Rearward from the leading edge, the Mach number in each case rises more or less rapidly to the prescribed value of unity on the forward side of the ridge. Turning the corner at the ridge, the flow expands discontinuously to a supersonic Mach number which, for given values of t/c and γ, is independent of conditions in the free stream. Over the rear half of the airfoil, the Mach number decreases slightly as a result of the compression waves reflected from the sonic line (see sketch on page 6). In general, for an airfoil of fixed thickness ratio, increasing the free-stream Mach number from unity brings about an increase in the average local Mach number over both the front and rear surfaces of the profile.

The nature of this latter variation is illustrated more clearly in figure 4, which is a cross plot of ξ versus ξ_0 for the 25- and 75-percent chordwise stations. The short vertical lines labelled S at $\xi_0 = 1.260$ denote the point at which the transonic small-disturbance theory predicts an attached bow wave with uniform sonic flow over the forward half of the profile. Results at this point and at all points to the right of S can be determined analytically as explained earlier in the text. It is apparent from figure 4 that the values given by the present numerical work satisfactorily bridge the gap which would otherwise exist between the analytical results at either side.

As can be seen from figure 4, the change in local conditions with change in free-stream Mach number is slight for a considerable distance away from a free-stream Mach number of 1. The curves of this figure have, in fact, been drawn with a horizontal tangent at $\xi_0 = 0$. This is in conformity with information which the authors have received from Gottfried Guderley concerning analytical results which he has recently obtained regarding flows with a free-stream Mach number close to 1. Guderley's results, which are yet to be published at the time this is written, indicate that just at the sonic flight speed the local Mach number at any point on an arbitrary two-dimensional profile is

stationary with respect to variations in the free-stream Mach number, that is,

$$\left(\frac{dM}{dM_o}\right)_{M_o=1} = 0 \tag{6}$$

In terms of the present variables (see equations (1) and (4)) this requires that

$$\left(\frac{d\xi}{d\xi_o}\right)_{\xi_o=0} = 0 \tag{7}$$

The same results were anticipated by Liepmann and Bryson on the basis of the physical considerations presented in reference 8.[6]

The pressure at a point in the generalized flow field of the small-disturbance theory is represented by the local value of a generalized pressure coefficient $\tilde{C}_p$ defined by the equation

$$\tilde{C}_p \equiv -2(\xi - \xi_o) \tag{8}$$

In transonic similarity considerations, $\tilde{C}_p$ is ordinarily related to the pressure coefficient $C_p \equiv (p-p_o)/q_o$ in an actual flow field by the approximate equation

$$\tilde{C}_p \cong \frac{(\gamma+1)^{1/3}}{(t/c)^{2/3}} C_p \tag{9}$$

At points on the surface of the airfoil, equation (5) applies for ξ, so that equation (8) there has the form

$$\tilde{C}_p = \tilde{C}_p\left(\frac{x}{c}, \xi_o\right) \tag{10}$$

The values of $\tilde{C}_p$ for the double-wedge section, as calculated from equation (8), are shown in figure 5. The curves here are essentially the same as the curves of ξ in figure 3, except that they are inverted and shifted vertically by an amount which differs for each curve. It can be seen from this figure that as the free-stream Mach number increases above 1 the pressure distribution tends toward the well-known supersonic type of distribution in which the pressure is uniform over each surface of the airfoil.

[6] The considerations of Liepmann and Bryson appear to be quite general with regard to the shape of the body or to the number of dimensions which characterize the flow field. Whether or not the results have in fact such wide validity is at present an open question.

Pressure Drag

Let the ordinates of the profile be given by $y/c = (t/c)\, f(x/c)$. With this notation, the pressure drag can be represented in the present theory by a generalized drag coefficient $\tilde{c}_d$ defined by the equation

$$\tilde{c}_d \equiv \oint \tilde{C}_p\left(\frac{x}{c}, \xi_o\right) f'\left(\frac{x}{c}\right) d\left(\frac{x}{c}\right) = \tilde{c}_d(\xi_o) \tag{11}$$

where $f'(x/c)$ is the derivative of $f(x/c)$ with respect to its argument and the integration is performed around the profile in the clockwise direction. According to the usual transonic similarity considerations, $\tilde{c}_d$ can be related to the actual drag coefficient c_d by the approximate relation

$$\tilde{c}_d \cong \frac{(\gamma+1)^{1/3}}{(t/c)^{5/3}}\, c_d \tag{12}$$

For the front half of the present profile, the ordinates are given by $y/c = \pm(t/c)(x/c)$ and equation (11) becomes

$$\tilde{c}_{d_f} = 2\int_0^{1/2} \tilde{C}_p\, d\left(\frac{x}{c}\right) \tag{13a}$$

where, because of symmetry, the integration need be performed over only the upper surface of the section. For the rear half, the ordinates are given by $y/c = \pm(t/c)(1-x/c)$ and equation (11) reduces to

$$\tilde{c}_{d_r} = -2\int_{1/2}^{1} \tilde{C}_p\, d\left(\frac{x}{c}\right) \tag{13b}$$

In the present study the integrals were evaluated by mechanical integration of the pressure-distribution curves of figure 5. In the case of $\tilde{c}_{d_f}$, a small, analytically determined allowance was included for the effect of the singularity at the leading edge. The final results are shown in figure 6. The drag coefficient of the complete airfoil was obtained, of course, by adding the drag coefficients for the front and rear wedges.

The results of figure 6 indicate that at a flight Mach number of 1 approximately two-thirds of the drag of the section is contributed by the rear half of the profile. As the Mach number increases from 1, the drag coefficient of the rear wedge is seen to decrease continuously. At the same time, the drag coefficient of the front wedge first increases

until it is considerably above that of the rear half, after which it also decreases. At a sufficiently high free-stream Mach number, the drag coefficient of each half of the airfoil is essentially the same. As a result of the difference in the drag variation of the two halves, the drag coefficient of the complete profile shows little variation for some distance above a Mach number of 1. As the shock wave attaches to the leading edge, however, and the local flow becomes everywhere supersonic, the total drag coefficient drops markedly. Far into the supersonic regime the variation is again less rapid. As will be seen, these statements may require some modification when applied to a specific airfoil, particularly with reference to the behavior of the total drag near the sonic flight speed. The curve for the front wedge in figure 6 can be continued into the subsonic range of flight speeds ($\xi_0<0$) by means of recent analytical work of Cole (to be published in the Jour. of Math. and Phys.). The continued curve decreases monotonically toward zero as the value of ξ_0 is reduced. Because of mathematical difficulties discussed by Cole, the continuation of the curve for the rear wedge into the subsonic range has not yet been accomplished. This curve would apparently reach a maximum at some subsonic flight condition and then also decrease toward zero.

As shown by Liepmann and Bryson (reference 8), the slope which the curves of figure 6 should have at the vertical axis can be determined from the previous results regarding the behavior of the local Mach number at the sonic flight condition. For example, taking the derivative of equation (13a) with respect to ξ_0, we write for the front wedge

$$\left(\frac{d\tilde{c}_{d_f}}{d\xi_0}\right)_{\xi_0=0} = 2\int_0^{1/2}\left(\frac{d\tilde{C}_p}{d\xi_0}\right)_{\xi_0=0} d\left(\frac{x}{c}\right) \tag{14}$$

But it follows from equation (8) that

$$\left(\frac{d\tilde{C}_p}{d\xi_0}\right)_{\xi_0=0} = -2\left[\left(\frac{d\xi}{d\xi_0}\right)_{\xi_0=0} - 1\right]$$

and hence, by virtue of equation (7), that

$$\left(\frac{d\tilde{C}_p}{d\xi_0}\right)_{\xi_0=0} = 2$$

Substitution of this value into equation (14) leads to the final result

$$\left(\frac{d\tilde{c}_{d_f}}{d\xi_0}\right)_{\xi_0=0} = 2 \tag{15a}$$

This is the result given previously by Liepmann and Bryson. The analogous relation for the rear wedge, obtained by proceeding from equation (13b), is

$$\left(\frac{d\tilde{c}_{d_r}}{d\xi_o}\right)_{\xi_o = 0} = -2 \tag{15b}$$

The curves for the front and rear halves of the airfoil in figure 6 thus have equal but opposite slopes where they meet the vertical axis. It follows at once that the curve for the complete airfoil has zero slope at the same point, that is, $(d\tilde{c}_d/d\xi_o)_{\xi_o = 0} = 0$.[7]

It will be noted that figure 6 also includes curves obtained from the standard supersonic small-disturbance theory. That such results can be included in a transonic similarity plot of this kind has been shown by several writers (see, for example, reference 17). In the case of the present profile, the drag coefficient of the complete section as given by the supersonic small-disturbance theory is (see page 154 of reference 19)

$$c_d = 4\,\frac{(t/c)^2}{(M_o^2-1)^{1/2}} \tag{16}$$

If both sides are multiplied by $(\gamma+1)^{1/3}/(t/c)^{5/3}$, this equation can be written

$$\frac{(\gamma+1)^{1/3}}{(t/c)^{5/3}}\,c_d = 4\,\frac{[(\gamma+1)(t/c)]^{1/3}}{(M_o^2-1)^{1/2}}$$

or, by virtue of equation (1),

$$\frac{(\gamma+1)^{1/3}}{(t/c)^{5/3}}\,c_d \cong \frac{4}{\xi_o^{1/2}} \tag{17}$$

Comparison of this equation with equation (12) shows that the results of the supersonic theory for the complete airfoil can be represented in a transonic similarity plot by the curve $\tilde{c}_d = 4/\xi_o^{1/2}$. Since the front

[7] In an earlier report of limited circulation, the curve of reduced drag coefficient for the complete airfoil was faired with a slightly positive slope at $\xi_o = 0$. This fairing was made before the results of the foregoing equations were known and was dictated by the results of the calculations as they stood at that time. The accuracy of the numerical work has since been improved through careful reduction in the truncation error. The present calculated points are completely consistent with the analytically determined slopes at $\xi_o = 0$.

and rear of the airfoil contribute equal drag in the supersonic theory, the corresponding results for the two halves can both be represented by the single curve $\tilde{c}_{d_f} = \tilde{c}_{d_r} = 2/\xi_0^{1/2}$. The dashed curves of figure 6 have been drawn in accordance with these relations.

For the rear half of the airfoil, the two theories illustrated in figure 6 are in reasonable agreement down to well within the regime of transonic flow. This result might not be anticipated, since the supersonic small-disturbance theory is based on the assumption of supersonic flow throughout the flow field. It is probably associated in some way with the fact that the local flow over the entire rear half of the airfoil remains supersonic (and nearly uniform) even after the flow over the front has become subsonic. For the front wedge, the results of the two theories diverge markedly even before the transonic regime is reached. The same is true of the curves for the complete airfoil. Within the transonic regime itself, the two theories give radically different results for both the front wedge and the complete airfoil. Near $\xi_0=0$ the two sets of results for the rear wedge are also completely different. This basic disagreement is a reflection of the fact that the supersonic theory is inherently incapable of dealing with problems involving mixed flows.

APPLICATION TO A SPECIFIC AIRFOIL

In the present section, the generalized curves of figure 6 will be used to obtain drag results for a specified value of t/c. This is done with the twofold purpose of providing some idea of numerical magnitudes for a representative specific case and of illustrating a certain indeterminacy which is encountered when the transonic small-disturbance theory is applied to airfoils of finite thickness. The numerical results will be prefaced by some general remarks concerning the nature of the information afforded by the small-disturbance theory.

General Considerations

The indeterminacy to be considered here derives from the fact that the transonic small-disturbance theory, though developed for vanishingly thin airfoils at free-stream Mach numbers infinitesimally close to 1, must be used in practice to provide results for airfoils of finite thickness at Mach numbers a finite distance from 1. Situations of this kind arise, of course, in any small-disturbance theory and bring with them questions which cannot be answered within the framework of the theory itself. The nature of the indeterminacy in the present theory is most easily illustrated by reference to the adiabatic energy equation. This equation is essential to the theory as a means of expressing the

local Mach number in terms of the local velocity and the so-called critical velocity. Before the small-disturbance approximation is introduced, the energy equation can be written in the well-known form

$$M^2 = \frac{2\left(\frac{u^2+v^2}{a_*^2}\right)}{(\gamma+1)-(\gamma-1)\left(\frac{u^2+v^2}{a_*^2}\right)} \tag{18}$$

where M is the local Mach number; u and v are the horizontal and vertical components, respectively, of the local velocity; and a_* is the critical velocity, that is, the velocity at which the velocity of flow and the velocity of sound are equal. In accordance with the basic assumption of the transonic small-disturbance theory (see page 9), the velocity components u and v are written

$$u = a_*\left[1 + \left(\frac{u}{a_*} - 1\right)\right]$$
$$v = a_*\theta$$

where the dimensionless disturbance velocity u/a_*-1 and the stream inclination θ are both small compared with 1. Substituting these expressions into equation (18) and discarding the second-order terms in u/a_*-1 and θ, one can write the energy equation for the transonic small-disturbance theory in the alternative forms

$$\left.\begin{matrix}\frac{M^2-1}{\gamma+1} \\ \frac{2(M-1)}{\gamma+1}\end{matrix}\right\} \cong \left\{\begin{matrix}\frac{u}{a_*} - 1 \\ \frac{1}{2}\left[\left(\frac{u}{a_*}\right)^2 - 1\right]\end{matrix}\right. \tag{19}$$

The braces here indicate that, to the order of accuracy of the present theory, either of the terms on one side of the equation may be set equal to either of the terms on the opposite side.[8] In the limit as $M \longrightarrow 1$ and $u/a_* \longrightarrow 1$, the various forms of equation (19) are, of course, identical. Since the assumptions of the small-disturbance theory imply such a limiting process, it is immaterial from the mathematical point of view which of the various forms is employed in the theoretical

[8]Actually, an infinity of equivalent terms can be obtained on each side by multiplication on the left by $[(M+1)/2]^m \cong 1$ and on the right by $[(u/a_*+1)/2]^n \cong 1$, where m and n are any positive or negative numbers. The terms written in equation (19), however, are the only ones which will be considered here.

development. Where M and u/a_* differ from 1 by a finite amount, however, as will be true in any practical case, the various forms of equation (19) are only approximate equalities; and a certain numerical indeterminacy will exist in the calculation of corresponding values of the two variables. From the practical point of view, therefore, the question of which form of equation (19) is employed is a matter of some importance.

The indeterminacy noted in the energy equation is reflected in other equations of the transonic small-disturbance theory. For example, the speed function ξ, which was previously given in a single form in equation (4), can, in view of equation (19), be represented equally well by the alternative expressions

$$\xi \cong \frac{M^2 - 1}{[(\gamma+1)(t/c)]^{2/3}} \cong \frac{2(M-1)}{[(\gamma+1)(t/c)]^{2/3}}$$

$$\cong \frac{(\gamma+1)^{1/3}}{(t/c)^{2/3}}\left[\frac{u}{a_*} - 1\right] \cong \frac{(\gamma+1)^{1/3}}{2(t/c)^{2/3}}\left[\left(\frac{u}{a_*}\right)^2 - 1\right] \qquad (20)$$

By the same token, the transonic similarity parameter ξ_0, previously given in equation (1), can be written alternatively as

$$\xi_0 \cong \frac{M_0^2 - 1}{[(\gamma+1)(t/c)]^{2/3}} \cong \frac{2(M_0 - 1)}{[(\gamma+1)(t/c)]^{2/3}}$$

$$\cong \frac{(\gamma+1)^{1/3}}{(t/c)^{2/3}}\left[\frac{u_0}{a_*} - 1\right] \cong \frac{(\gamma+1)^{1/3}}{2(t/c)^{2/3}}\left[\left(\frac{u_0}{a_*}\right)^2 - 1\right] \qquad (21)$$

With regard to the use of these alternative expressions, two points of view must again be distinguished: (a) From the point of view of the mathematical derivation, which presupposes that $t/c \longrightarrow 0$ and $M \longrightarrow 1$, the alternative expressions of equation (20) constitute indeterminate forms of the type 0/0. At any given location, all these indeterminate forms have the identical limiting value ξ. Analogous observations can be made, of course, with regard to equation (21). Mathematically speaking, therefore, the equation $\xi = \xi\left(\frac{x}{c}, \xi_0\right)$, given earlier as equation (5), provides a functional relationship between the limiting values of two indeterminate forms, each of which can be expressed in several wholly equivalent ways. Only in this limiting sense can the small-disturbance theory be said to provide a unique result for the flow over a given type of profile. (b) In practical application, the alternative expressions of equations (20) and (21) must be regarded as quotients of two small but finite quantities, and the equations themselves as only approximate equalities. From the practical point of view, therefore, the quantitative relationship between the Mach number on the

airfoil and the Mach number in the free stream will depend upon which form of equations (20) and (21) is chosen for substitution into the relation between ξ and ξ_o. For this reason, the small-disturbance theory will not provide in actual use a unique result for the distribution of Mach number over a given airfoil for given values of t/c and M_o.

An indeterminacy of a slightly different nature arises in the computation of the pressure coefficient.[9] The basic assumptions of the small-disturbance theory imply not only that the local velocity and the free-stream velocity differ only slightly from the critical velocity but also that the local velocity and free-stream velocity differ only slightly from each other. On the basis of this last implication, the pressure coefficient $C_p \equiv (p-p_o)/q_o$ can be approximated by the following relation, well-known from the small-disturbance theories of completely subsonic or supersonic flow:

$$C_p \cong -2\frac{u-u_o}{u_o} \tag{22a}$$

By setting $u_o = a_* + (u_o - a_*)$ in the denominator, carrying out the division, and neglecting terms of higher than the first order of smallness, one can write equally well in the present theory

$$C_p \cong -2\frac{u-u_o}{a_*} \tag{22b}$$

These two expressions are obviously identical in the limit as $u_o/a_* \longrightarrow 1$. They are thus completely equivalent insofar as the mathematics of the theory is concerned. In any practical application, however, the quantitative results will again depend on which expression is used. Taking equation (22b) first, if this equation is rewritten as

$$C_p \cong -2\left[\left(\frac{u}{a_*}-1\right)-\left(\frac{u_o}{a_*}-1\right)\right]$$

and substitution is made from the appropriate form of equations (20) and (21), then one obtains for the pressure coefficient

$$\frac{(\gamma+1)^{1/3}}{(t/c)^{2/3}}C_p = -2(\xi-\xi_o)$$

[9] This indeterminacy was first pointed out to the authors by Hans W. Liepmann.

With the previous definition of the generalized pressure coefficient $\tilde{C}_p \equiv -2(\xi - \xi_o)$ (see equation (8)), this becomes

$$\frac{(\gamma+1)^{1/3}}{(t/c)^{2/3}} C_p \cong \tilde{C}_p \tag{23}$$

This is the relation given earlier as equation (9). If equation (22a) is used for C_p, then one writes

$$C_p \cong -2\frac{u-u_o}{u_o} = -2\frac{u-u_o}{a_*} \times \frac{a_*}{u_o}$$

which gives finally, with the aid of the third form of equation (21),

$$\frac{(\gamma+1)^{1/3}}{(t/c)^{2/3}} C_p \cong \left[1 - \frac{(t/c)^{2/3}}{(\gamma+1)^{1/3}} \xi_o\right] \tilde{C}_p \tag{24}$$

In the limit as $t/c \longrightarrow 0$, equation (24) reduces to equation (23), which is the form commonly used in transonic similarity considerations. Using equation (24) for the practical calculation of the pressure coefficient is thus equivalent to arbitrarily retaining a higher-order term in t/c in the computations. This is perhaps inconsistent with the mathematical procedures used in developing the theory, but it may have certain advantages from the practical point of view. The nature of these possible advantages will be discussed later.

To obtain the drag coefficient, the pressure coefficient is integrated in the clockwise direction around the section according to the equation

$$c_d = \oint C_p \, d\left(\frac{y}{c}\right) \tag{25}$$

With section ordinates given by $y/c = (t/c) f(x/c)$ as before, this equation becomes

$$c_d = \frac{t}{c} \oint C_p \, f'\left(\frac{x}{c}\right) d\left(\frac{x}{c}\right)$$

Substituting for C_p from equation (23) and utilizing the previous definition (11) for the generalized drag coefficient $\tilde{c}_d$ gives finally

$$\frac{(\gamma+1)^{1/3}}{(t/c)^{5/3}} c_d \cong \tilde{c}_d$$

which is the result cited earlier as equation (12). Equation (26) is the relation ordinarily used in transonic similarity considerations. If equation (24) is used for C_p instead of equation (23), one obtains in place of equation (26)

$$\frac{(\gamma+1)^{1/3}}{(t/c)^{5/3}} c_d \cong \left[1 - \frac{(t/c)^{2/3}}{(\gamma+1)^{1/3}} \xi_o\right] \tilde{c}_d \qquad (27)$$

As before, this equation reduces to the previous form as $t/c \longrightarrow 0$.

Variation of Drag Coefficient With Mach Number

As is apparent from the foregoing remarks, various procedures are possible in applying the results of the small-disturbance theory to an airfoil of given t/c. In the remainder of the report, these procedures will be discussed with reference to the variation of drag coefficient with free-stream Mach number. Similar considerations would apply, however, with regard to the variation in pressure coefficient at a point on the surface of the airfoil. The value of t/c to be used in the discussion will be taken as 0.0787, which is the value corresponding to the thinnest wedge tested by Liepmann and Bryson (semiangle of wedge = $4\text{-}1/2^\circ$). The value of γ will be taken as 1.4, the value commonly used for air.

The final results for the selected thickness ratio are given in figure 7, in which the pressure drag coefficient of the front wedge, the rear wedge, and the complete profile are shown as functions of the Mach number in three separate plots. In each plot, four full curves are shown, all derived from the basic transonic small-disturbance results of figure 6. For the two upper curves in each case, the drag coefficients were computed by means of the elementary equation (26). For this pair of curves, the Mach numbers for the curve to the right were computed from the form of equation (21) containing $(M_o - 1)$; the Mach numbers for the curve to the left from the form containing $(M_o^2 - 1)$. For the two lower curves in each plot the drag coefficients were determined from equation (27), which retains the higher-order term in t/c. The Mach numbers here were computed in the same way as for the previous pair of curves. In addition to the foregoing results, each part of figure 7 also includes a curve calculated according to the standard shock-expansion theory (see, for example, reference 20). This theory, which is based on a stepwise application of the complete equations for an oblique shock wave and a Prandtl-Meyer expansion, applies only in the range in which the shock-wave equations predict an attached wave with not less than sonic velocity on the downstream side. Except for a very small error in the drag of the rear wedge near the low end of this range (see footnote 5), the shock-expansion theory provides the exact inviscid solution for the present profile. Also contained in figure 7

are curves given by the supersonic small-disturbance theory (as, for example, by equation (16)). The results shown in this figure are representative, qualitatively speaking, of those which are obtained for other values of t/c.

On the basis of figure 7, it is possible to assess the relative merit of the various procedures for applying the transonic small-disturbance theory to airfoils of finite thickness. This can be done by comparing the results given by the various procedures with the results given by more rigorous methods in the regions where such methods are available. It was hoped originally that such a comparison would show one of the procedures to be definitely superior to all of the others. The results of figure 7 show, unfortunately, that the situation is not that simple. The details are worth discussing at some length, since the present work affords one of the first rigorous quantitative applications of the transonic small-disturbance theory at other than the sonic flight condition.

As a basis for the discussion, the earlier considerations regarding the rate of change of the drag coefficient at the sonic flight speed must first be extended to airfoils of finite thickness. As previously implied, the analytical results of Guderley regarding conditions at a free-stream Mach number of 1 (see page 15) do not of themselves require the assumption that $t/c \longrightarrow 0$. (The same observation can also be made with reference to the physical considerations of Liepmann and Bryson.) This means that the result of equation (6) — namely, that $(dM/dM_o)_{M_o=1} = 0$ — is not restricted to airfoils of vanishing thickness but may be applied in cases of finite thickness as well. On the basis of this result, it is, in fact, a simple matter to obtain exact relations for the slope of the drag curves at a free-stream Mach number of 1 (see appendix for details). The final equations, which are the only items of importance here, are as follows:

For the front wedge

$$\left(\frac{dc_{d_f}}{dM_o}\right)_{M_o = 1} = \frac{4}{\gamma+1}\left(\frac{t}{c}\right) - \frac{2}{\gamma+1}\left(c_{d_f}\right)_{M_o = 1} \tag{28a}$$

For the rear wedge

$$\left(\frac{dc_{d_r}}{dM_o}\right)_{M_o = 1} = -\frac{4}{\gamma+1}\left(\frac{t}{c}\right) - \frac{2}{\gamma+1}\left(c_{d_r}\right)_{M_o = 1} \tag{28b}$$

For the complete airfoil

$$\left(\frac{dc_d}{dM_o}\right)_{M_o = 1} = -\frac{2}{\gamma+1}\left(c_d\right)_{M_o = 1} \tag{28c}$$

Each of these relations is seen to contain a negative term which is proportional in value to the drag coefficient itself. As pointed out in the appendix, this term is the result of a relative variation between the dynamic pressures in the free stream and at the sonic point. The other term which appears in the equations for the front and rear wedges is associated with a relative variation between the corresponding static pressures. This term is of opposite sign for the two halves of the airfoil so that it disappears in the final equation for the complete profile. The most significant final result is that the exact theoretical curve for the pressure drag of the complete airfoil must have a negative slope at a free-stream Mach number of 1.[10]

The foregoing exact equations provide a standard against which to compare the various procedures used to obtain the approximate transonic curves of figure 7. Equation (26), which is the basis for the two upper curves in each part of the figure, will be considred first. Differentiation of this equation and application of the results of equations (15a) and (15b) leads to the following approximate equations[11] for the slope of the drag curve at $M_o = 1$:

For the front wedge

$$\left(\frac{dc_{d_f}}{dM_o}\right)_{M_o=1} \cong \frac{4}{\gamma+1}\left(\frac{t}{c}\right) \tag{29a}$$

For the rear wedge

$$\left(\frac{dc_{d_r}}{dM_o}\right)_{M_o=1} \cong -\frac{4}{\gamma+1}\left(\frac{t}{c}\right) \tag{29b}$$

For the complete airfoil

$$\left(\frac{dc_d}{dM_o}\right)_{M_o=1} \cong 0 \tag{29c}$$

These results differ from the exact equations (28) by the omission in each case of the term which is proportional to the drag coefficient. The slope of the upper pair of curves in each part of figure 7 conforms with these approximate relations.

Equation (27), which is the basis for the lower pair of curves in each plot, provides a different result. Differentiation of this equation

[10]This fact was brought to the authors' attention by Gottfried Guderley.

[11]It is immaterial here which form of equation (21) is used for the necessary relation between ξ_o and M_o.

can readily be shown to lead, in fact, to slope equations identical in form with the exact equations (28). The slope of the lower pair of curves in each part of figure 7 conforms with these exact relations.

It appears from the foregoing results that the simple equation (26), which neglects all higher-order terms in t/c, takes proper account near the sonic flight speed of the relative variation between the static pressures in the free stream and at the sonic point. It fails, however, to reflect the variation in the corresponding dynamic pressures. Because of this deficiency, the curves based on equation (26) fail, in particular, to show the proper negative slope for the pressure drag coefficient of the complete airfoil at $M_o = 1$. The shortcomings of equation (26) in this regard can be overcome rather simply by using in its place an equation such as (27) in which an appropriate higher-order term in t/c is arbitrarily retained. The slopes of the curves given by this equation at $M_o = 1$, in fact, fall short of being completely exact only by the fact that the drag coefficients $(c_{d_f})_{M_o=1}$, etc., which appear on the right-hand side of the slope equations are not known exactly for the given t/c. It appears, therefore, that equation (27), though somewhat arbitrary from the theoretical point of view, is to be preferred for the computation of the drag of an airfoil of finite thickness near $M_o = 1$.

Near the upper end of the transonic regime, where the presence of the shock-expansion curve provides a second opportunity for comparison between the exact and approximate theories, the situation is less clear cut. To examine the circumstances here, it is not appropriate to compare values of the drag coefficient at a given Mach number since, at certain Mach numbers, the points on the various curves would then correspond to essentially different regimes of flow. A more meaningful procedure is to make a separate comparison of both the drag and the Mach number at the various points which correspond to uniform sonic flow over the forward half of the profile. As in the earlier figures, these points are denoted in figure 7 by the letter S.

First, with regard to the drag coefficient at the points S, it is apparent that the simple equation (26), which neglects all higher-order terms in t/c, overestimates the drag of the front wedge at this flow condition by about 12 percent. The more complicated equation (27), which retains a higher-order term, underestimates this drag by a somewhat lesser amount. For the rear wedge, equation (27) gives a value which is in almost exact agreement with the shock-expansion value, while equation (26) gives a value which is approximately 19 percent too high. For the complete airfoil, the net error in the pressure drag is about −5 percent by equation (27) and +14 percent by equation (26).

With regard to the Mach number M_o at the points S, it is seen from figure 7 that both the first and second forms of equation (21) predict too low a Mach number for the attainment of uniform sonic flow

over the forward surface of the profile. The second form – that is, the form involving (M_o-1) – is the least inaccurate in this regard. The discrepancy with even this form, however, is still significant for an airfoil of the present thickness.

To summarize the discussion of the foregoing paragraphs, it appears that equation (27), which retains the higher-order term in t/c, has certain advantages over the simpler equation (26) for determining the variation of drag coefficient with Mach number for an airfoil of finite thickness. These advantages are particularly evident at free-stream Mach numbers close to 1; they are less evident, though still present, at Mach numbers approaching the regime of purely supersonic flow. The most troublesome point in the application of the results of the small-disturbance theory to airfoils of finite thickness appears to be in the determination of the free-stream Mach number at which the calculated drag coefficient applies. For Mach numbers some distance removed from 1, both of the pertinent forms of equation (21) give values of M_o which are erroneously low. Because of this deficiency, the over-all curves based on equation (27), though probably of good accuracy at Mach numbers close to 1, lie considerably below the more accurate shock-expansion curve in the regime of purely supersonic flow. In this regime, in fact, the curves obtained from equation (26) appear to give the better agreement with the shock-expansion results. This agreement is, however, the result of compensating errors in the drag coefficient and Mach number and is therefore largely illusory. In view of the possible advantages of equation (27) at the lower Mach numbers, this seeming agreement on the basis of equation (26) might be expected to disappear rather quickly if the shock-expansion curve could be extended into the transonic regime with undiminished accuracy.

In light of the foregoing results, it is hardly possible to recommend any single procedure for applying the results of the small-disturbance theory to airfoils of finite thickness. Other methods than those illustrated here can, of course, be tried – there are, in fact, an infinite number of possibilities, all equally valid from the mathematical point of view. There is little to be gained, however, by complicating matters any further. For airfoils thinner than the one chosen here, the discrepancies between the various results become rapidly smaller and can be neglected. For airfoils of thickness equal to or greater than that used in figure 7, an interpolated curve which should be accurate enough for most practical purposes can be obtained by extending the shock-expansion curve judiciously into the transonic regime, using the results of the transonic small-disturbance theory as a guide. In the absence of exact knowledge of the drag coefficient at $M_o=1$, this curve would be drawn through the point given by Guderley and Yoshihara with an appropriate local slope as given by one of the exact equations (28). A possible curve of this type is included, for example, in figure 7(c). Since the effects of finite span will be to reduce the drag at transonic speeds, such an interpolated curve may be looked upon as providing an approximate upper bound for the inviscid pressure drag

of a three-dimensional wing. In fact, until some knowledge is obtained regarding the effects of finite span and fluid viscosity, it is doubtful if more accurate two-dimensional, inviscid calculations for thin double-wedge profiles would be worth the trouble from an engineering point of view. In the present state of theoretical development, knowledge of these effects will probably have to come from experiment.

CONCLUDING REMARKS

The results of the present numerical analysis show the salient features of the two-dimensional inviscid flow over a thin, doubly symmetrical, double-wedge profile in the range of supersonic flight speeds in which the bow wave is detached. The most important findings are summarized in the following paragraphs:

1. The vertical extent of the subsonic region behind the detached wave is large even when the wave is only a relatively small distance removed from the leading edge. This implies that the tip effects may be large on finite-span wings when the bow wave is detached.

2. The local Mach number M at a point on the surface of the airfoil increases monotonically as the free-stream Mach number M_o increases from 1. The increase in M is at first very slight for a considerable increment away from the sonic flight condition. This confirms previous findings that the local Mach number has a stationary value at $M_o = 1$ and shows that these findings provide a good working approximation even at Mach numbers a short distance removed from 1. When considered in terms of the pressure coefficient on the surface of the airfoil, the results show how the transonic pressure distribution tends, as the flight Mach number increases, toward the purely supersonic type of distribution known to exist in the upper portion of the speed range.

3. As the free-stream Mach number increases from 1, the pressure drag coefficient contributed by the front half of the airfoil increases until it reaches a maximum at a flight speed somewhat below that for which the bow wave attaches to the leading edge. It then decreases, the rate of the decrease being at first rapid in the vicinity of bow-wave attachment and then less rapid in the range of purely supersonic flow. The pressure drag coefficient contributed by the rear half of the airfoil decreases continuously over the entire supersonic range of flight speeds. This latter result indicates that the drag coefficient of the rear half must attain its maximum at a subsonic flight condition. Because of the differences in the drag variation for the two halves, the pressure drag of the complete airfoil varies relatively slightly near the sonic flight speed, decreases rapidly in the vicinity of bow-wave attachment, and then decreases at a progressively less rapid rate in the range of purely supersonic flow.

The results of the analysis also serve to illustrate the numerical indeterminacy which is encountered when the transonic small-disturbance theory is used to obtain quantitative results for airfoils of finite thickness at free-stream Mach numbers a finite distance from 1. It is shown, in particular, how various approximate curves of pressure drag coefficient versus Mach number for a given thickness ratio can be obtained by using equations which differ only to the order of terms neglected in the mathematical development of the theory. With these curves and the fragmentary results of more rigorous theories as a guide, an interpolated curve can be drawn which is probably as accurate as is practically justified in view of the fundamental disregard of tip effects and fluid viscosity. As required by the physical considerations of Liepmann and Bryson and by the mathematical findings of Guderley, such a curve for the complete profile would have a negative slope at a free-stream Mach number of 1.

Ames Aeronautical Laboratory,
National Advisory Committee for Aeronautics,
Moffett Field, Calif., Jan. 19, 1951.

APPENDIX

EXACT RELATIONS FOR SLOPE OF DRAG CURVE AT A FREE-STREAM MACH NUMBER OF 1

In the section APPLICATION TO A SPECIFIC AIRFOIL, exact relations are given for the slope of the curve of drag coefficient versus free-stream Mach number at a free-stream Mach number of 1. These relations are based, as explained in the text, on the fact that at the sonic flight condition the local Mach number M at the surface of an airfoil is stationary with respect to variations in the free-stream Mach number M_o – that is, $(dM/dM_o)_{M_o=1} = 0$. The details of the derivation are given in the following paragraphs. The results are not restricted to a double-wedge section but are applicable to the zero-lift drag of a symmetrical profile of any shape.

The general equation for the pressure coefficient, valid for any Mach number and thickness ratio, can be written as

$$C_p \equiv \frac{p-p_o}{q_o} = \frac{p-p_o}{q_*} \times \frac{q_*}{q_o} = \frac{2}{\gamma}\left(\frac{p}{p_*} - \frac{p_o}{p_*}\right)\frac{1}{q_o/q_*} \tag{A1}$$

where p is the static pressure at an arbitrary point on the airfoil, p_* and q_* are the static and dynamic pressures at the point on the airfoil at which $M = 1$, and p_o and q_o are the static and dynamic pressures in the free stream. When $M_o = 1$, conditions in the free stream and at the sonic point are obviously equal $\left(p_{o_{M_o=1}} = p_{*_{M_o=1}}, q_{o_{M_o=1}} = q_{*_{M_o=1}}\right)$ so that

$$C_{p_{M_o=1}} = \frac{2}{\gamma}\left[\left(\frac{p}{p_*}\right)_{M_o=1} - 1\right] \tag{A2}$$

Differentiation of equation (A1) with respect to M_o then gives for the rate of change of the pressure coefficient at $M_o = 1$

$$\left(\frac{dC_p}{dM_o}\right)_{M_o=1} = \frac{2}{\gamma}\left\{\left[\frac{d(p/p_*)}{dM_o}\right]_{M_o=1} - \left[\frac{d(p_o/p_*)}{dM_o}\right]_{M_o=1}\right\} - C_{p_{M_o=1}}\left[\frac{d(q_o/q_*)}{dM_o}\right]_{M_o=1} \tag{A3}$$

It is now necessary to evaluate the three derivatives on the right-hand side of this equation.

If there are no shock waves present on the surface of the airfoil, the ratio p/p_* can be expressed solely in terms of the local Mach number by an isentropic equation of the form

$$\frac{p}{p_*} = f(M)$$

where the exact nature of the function $f(M)$ is immaterial in the present application. From this equation and from the known fact that $(dM/dM_O)_{M_O=1} = 0$, it follows at once that

$$\left[\frac{d(p/p_*)}{dM_O}\right]_{M_O=1} = f'(M)\left(\frac{dM}{dM_O}\right)_{M_O=1} = 0 \qquad (A4)$$

If there are shock waves present on the airfoil, the argument is slightly more involved, but the same result applies. Equation (A4) states, in effect, that as the free-stream Mach number varies from unity the entire pressure distribution on the surface of the airfoil varies in direct proportion to the pressure at the sonic point.

The derivative $[d(p_O/p_*)/dM_O]_{M_O=1}$, which defines the relative variation between the static pressures in the free stream and at the sonic point, can be found by first expressing the ratio p_O/p_* in terms of the free-stream Mach number M_O. The necessary expression can be obtained obtained either from the equations for isentropic flow alone ($M_O < 1$, no shock wave ahead of the airfoil) or from these equations plus the equations for the normal shock wave ($M_O > 1$, detached wave ahead of airfoil). In either case, if the expression is expanded about $M_O = 1$ in terms of ascending powers of (M_O^2-1), the result is

$$\frac{p_O}{p_*} = 1 - \frac{\gamma}{\gamma+1}(M_O^2-1) + O[(M_O^2-1)^2]$$

Differentiation of this equation then gives

$$\left[\frac{d(p_O/p_*)}{dM_O}\right]_{M_O=1} = -\frac{2\gamma}{\gamma+1} \qquad (A5)$$

The derivative $[d(q_O/q_*)/dM_O]_{M_O=1}$, which defines the relative variation between the dynamic pressures in the free stream and at the sonic point, can be found by expressing q_O/q_* in terms of known quantities. The necessary relation is given by

$$\frac{q_O}{q_*} = \left(\frac{p_O}{p_*}\right) M_O^2$$

from which it follows that

$$\left[\frac{d(q_o/q_*)}{dM_o}\right]_{M_o=1} = \left[\frac{d(p_o/p_*)}{dM_o}\right]_{M_o=1} + 2 = \frac{2}{\gamma+1} \tag{A6}$$

The findings of equations (A4), (A5), and (A6) can now be substituted into the previous equation (A3). The result is the following important relation for the rate of change of the pressure coefficient at the sonic flight speed:

$$\left(\frac{dC_p}{dM_o}\right)_{M_o=1} = \frac{4}{\gamma+1} - \frac{2}{\gamma+1} C_{p_{M_o=1}} \tag{A7}$$

This relation is exact within the limitations of the inviscid theory and is applicable to an airfoil of any shape and thickness ratio.

The drag coefficient of the front portion of any symmetrical airfoil at zero lift can be written, by virtue of the general equation (25) of the main text, as

$$c_{d_f} = \int_{-\frac{(t/c)}{2}}^{\frac{(t/c)}{2}} C_p \, d\left(\frac{y}{c}\right)$$

where the integration is carried out over the surface forward of the position of maximum thickness. Differentiation of this equation with respect to M_o and substitution from equation (A7) gives, after integration,

$$\left(\frac{dc_{d_f}}{dM_o}\right)_{M_o=1} = \frac{4}{\gamma+1}\left(\frac{t}{c}\right) - \frac{2}{\gamma+1}\left(c_{d_f}\right)_{M_o=1} \tag{A8}$$

Similar reasoning gives for the rear portion of the airfoil

$$\left(\frac{dc_{d_r}}{dM_o}\right)_{M_o=1} = -\frac{4}{\gamma+1}\left(\frac{t}{c}\right) - \frac{2}{\gamma+1}\left(c_{d_r}\right)_{M_o=1} \tag{A9}$$

It follows that for the complete airfoil

$$\left(\frac{dc_d}{dM_o}\right)_{M_o=1} = -\frac{2}{\gamma+1}\left(c_d\right)_{M_o=1} \tag{A10}$$

These equations are given as equations (28) in the main body of the report. It is apparent from the foregoing derivation that the negative term proportional to the drag coefficient in each of these equations appears as a consequence of the relative variation between the dynamic pressures in the free stream and at the sonic point. The term proportional to t/c in equations (A8) and (A9) is a result of the relative variation between the corresponding static pressures.

REFERENCES

1. Meyer, Th.: Über zweidimensionale Bewegungsvorgänge in einem Gas, das mit Überschallgeschwindigkeit strömt. Forschungsarbeiten auf dem Gebiete des Ingenieurwesens, VDI, vol. 62, 1908, pp. 31-67.

2. Guderley, K. Gottfried: Considerations of the Structure of Mixed Subsonic-Supersonic Flow Patterns. Tech. Rep. No. F-TR-2168-ND, AAF, Air Materiel Command (Wright Field), Oct. 1947.

3. Maccoll, J.W., and Codd, J.: Theoretical Investigations of the Flow around Various Bodies in the Sonic Region of Velocities. Theo. Res. Rep. No. 17/45, Armament Res. Dept., British Ministry of Supply, Sept. 1945.

4. Maccoll, J.W.: Investigations of Compressible Flow at Sonic Speeds, Theo. Res. Rep. No. 7/46, Armament Res. Dept., British Ministry of Supply, Sept. 1946.

5. Frankl, F.: On the Problems of Chaplygin for Mixed Sub- and Supersonic Flows. NACA TM 1155, 1947.

6. Busemann, Adolf: A Review of Analytical Methods for the Treatment of Flows with Detached Shocks. NACA TN 1858, 1949.

7. Guderley, G., and Yoshihara, H.: The Flow over a Wedge Profile at Mach Number 1. Jour. Aero. Sci., vol. 17, no. 11, Nov. 1950, pp. 723-735.

8. Liepmann, H.W., and Bryson, A.E., Jr.: Transonic Flow Past Wedge Sections. Jour. Aero. Sci., vol. 17, no. 12, Dec. 1950, pp. 745-755.

9. Tricomi, F.: On Linear Partial Differential Equations of the Second Order of Mixed Type. Trans. A9-T-26, Grad. Div. of Appl. Math., Brown University, 1948.

10. Emmons, Howard W.: The Numerical Solution of Partial Differential Equations. Quarterly Appl. Math., vol. II, no. 3, Oct. 1944, pp. 173-195.

11. Fox, L.: A Short Account of Relaxation Methods. Quarterly Jour. Mech. and Appl. Math., vol. 1, pt. 3, Sept. 1948, pp. 253-280.

12. Shaw, F.S.: Numerical Solutions of Boundary Value Problems by Relaxation Methods. Numerical Methods of Analysis in Engineering, L. E. Grinter, ed., Macmillan Co., 1949, pp. 49-65.

13. Tsien, Hsue-Shen, and Baron, Judson R.: Airfoils in Slightly Supersonic Flow. Jour. Aero. Sci., vol. 16, no. 1, Jan. 1949, pp. 55-61.

14. von Kármán, Theodore: The Similarity Law of Transonic Flow. Jour. Math. and Phys., vol. XXVI, no. 3, Oct. 1947, pp. 182-190.

15. Kaplan, Carl: On Similarity Rules for Transonic Flows. NACA Rep. 894, 1948.

16. Liepmann, H.W., Ashkenas, H., and Cole, J.D.: Experiments in Transonic Flow. Tech. Rep. No. 5667, Air Materiel Command, U. S. Air Force, Feb. 1948.

17. Spreiter, John R.: Similarity Laws for Transonic Flows about Wings of Finite Span. NACA TN 2273, 1950.

18. Guderley, K. Gottfried: Singularities at the Sonic Velocity. Tech. Rep. F-TR-1171-ND, Air Materiel Command, U. S. Air Force, June 1948.

19. Liepmann, Hans Wolfgang, and Puckett, Allen E.: Introduction to Aerodynamics of a Compressible Fluid. John Wiley and Sons, Inc., 1947.

20. Ivey, H. Reese, Stickle, George W., and Schuettler, Alberta: Charts for Determining the Characteristics of Sharp-Nose Airfoils in Two-Dimensional Flow at Supersonic Speeds. NACA TN 1143, 1947.

BIBLIOGRAPHY

(Arranged chronologically)

1. Laitone, Edmund V., and Pardee, Otway O'M.: Location of Detached Shock Wave in Front of a Body Moving at Supersonic Speeds. NACA RM A7B10, 1947.

2. Lin, C. C., and Rubinov, S. I.: On the Flow Behind Curved Shocks. Jour. of Math. and Phys., vol. XXVII, no. 2, July 1948, pp. 105-129.

3. Munk, M.M., and Crown, J. Conrad: The Head Shock Wave. Naval Ordnance Lab. Memo 9773, Aug. 1948.

4. Drougge, Georg: The Flow around Conical Tips in the Upper Transsonic Range. Rep. No. 25, Flygtekniska Försöksanstalten (Stockholm), 1948.

5. Dugundji, John: An Investigation of the Detached Shock in Front of a Body of Revolution. Jour. Aero. Sci., vol. 15, no. 12, Dec. 1948, pp. 699-706.

6. Ferri, Antonio: Method for Evaluating from Shadow or Schlieren Photographs the Pressure Drag in Two-Dimensional or Axially Symmetrical Flow Phenomena with Detached Shock. NACA TN 1808, 1949.

7. Moeckel, W.E.: Approximate Method for Predicting Form and Location of Detached Shock Waves Ahead of Plane or Axially Symmetric Bodies. NACA TN 1921, 1949.

8. Perl, William: Calculation of Transonic Flows Past Thin Airfoils by an Integral Method. NACA TN 2130, 1950.

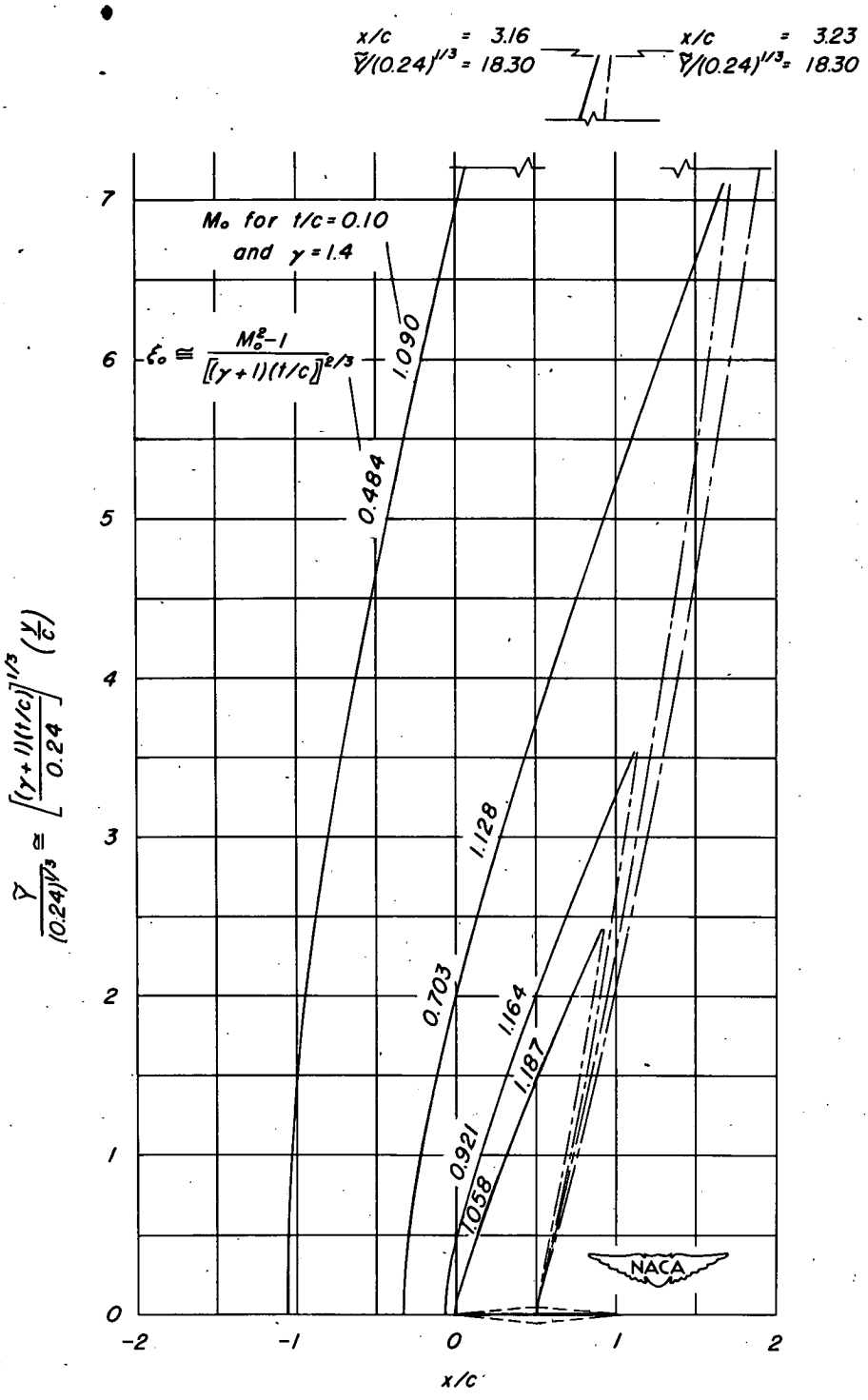

Figure 1.- Shape of bow wave and sonic line.

Page intentionally left blank

Page intentionally left blank

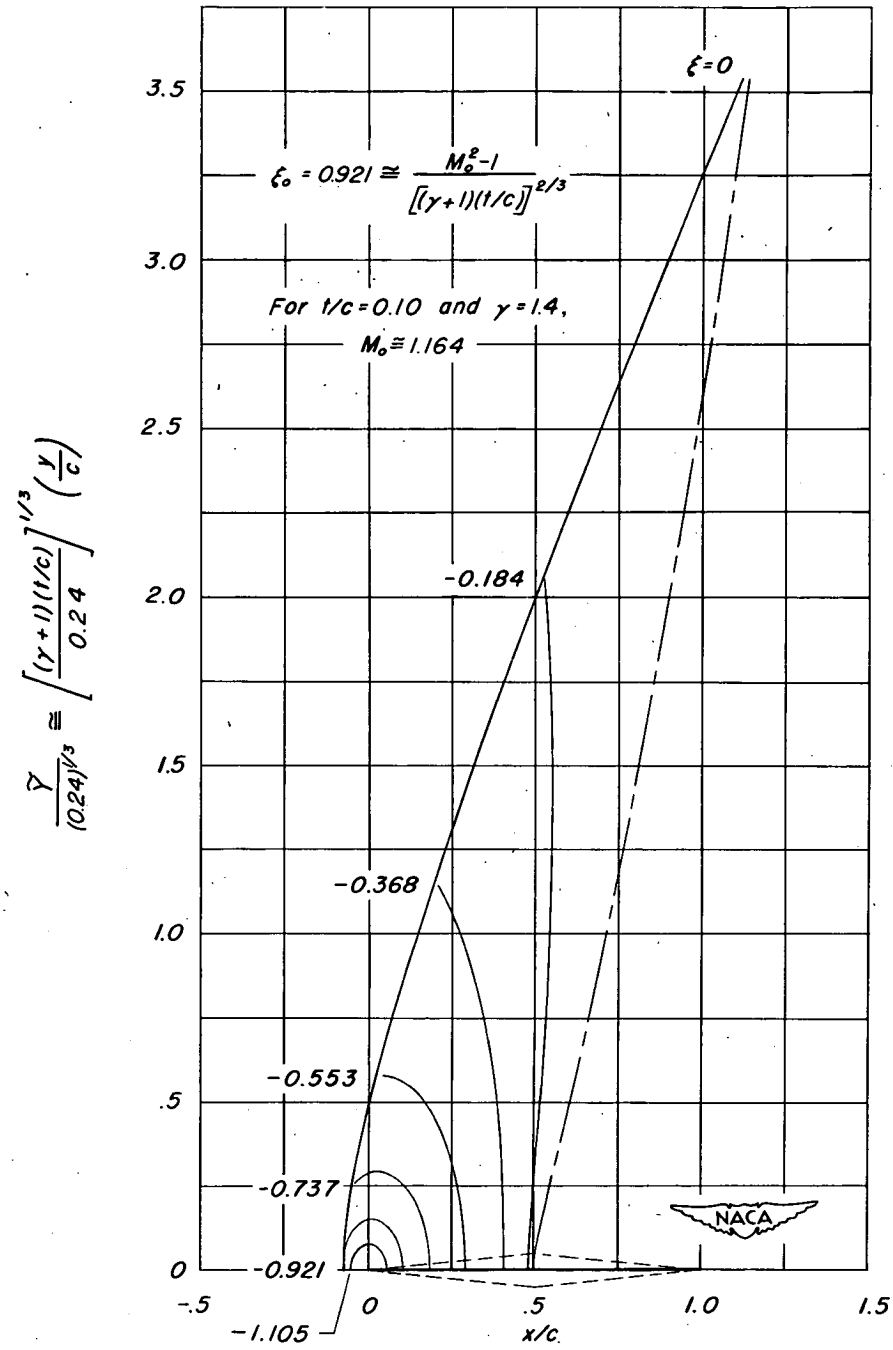

Figure 2.- Contours of constant speed function for $\xi_0 = 0.921$.

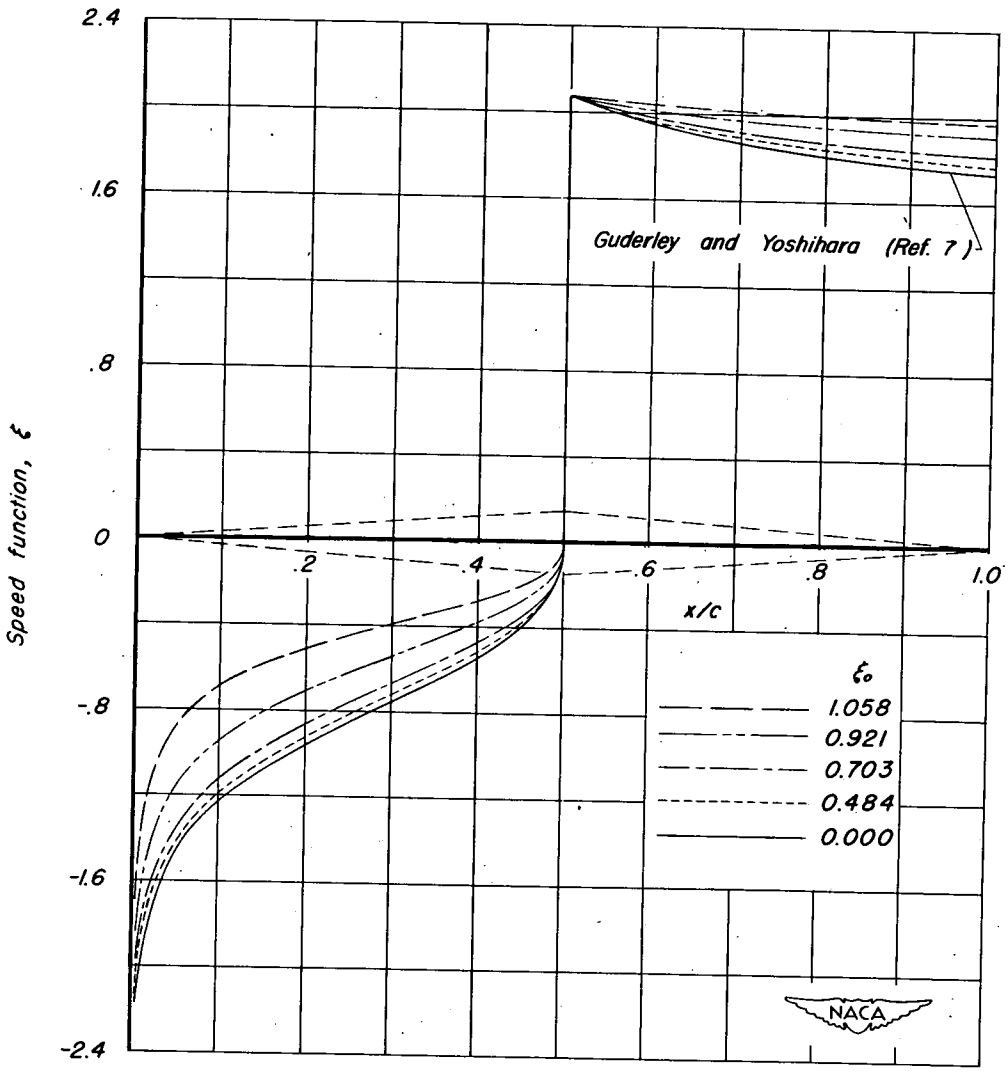

Figure 3.- Chordwise distribution of speed function at surface of airfoil.

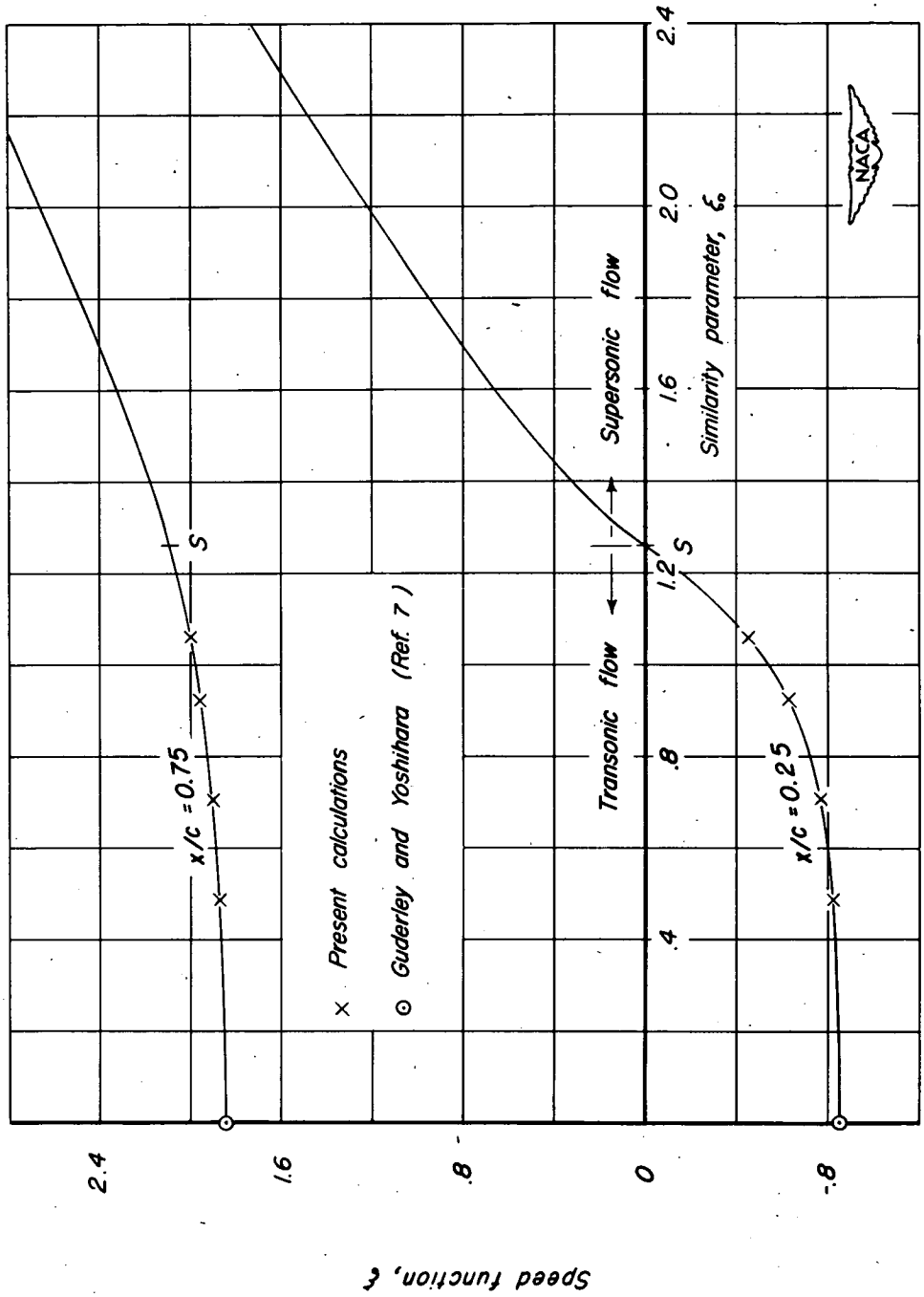

Figure 4.- Variation of speed function at 25- and 75- percent chordwise stations.

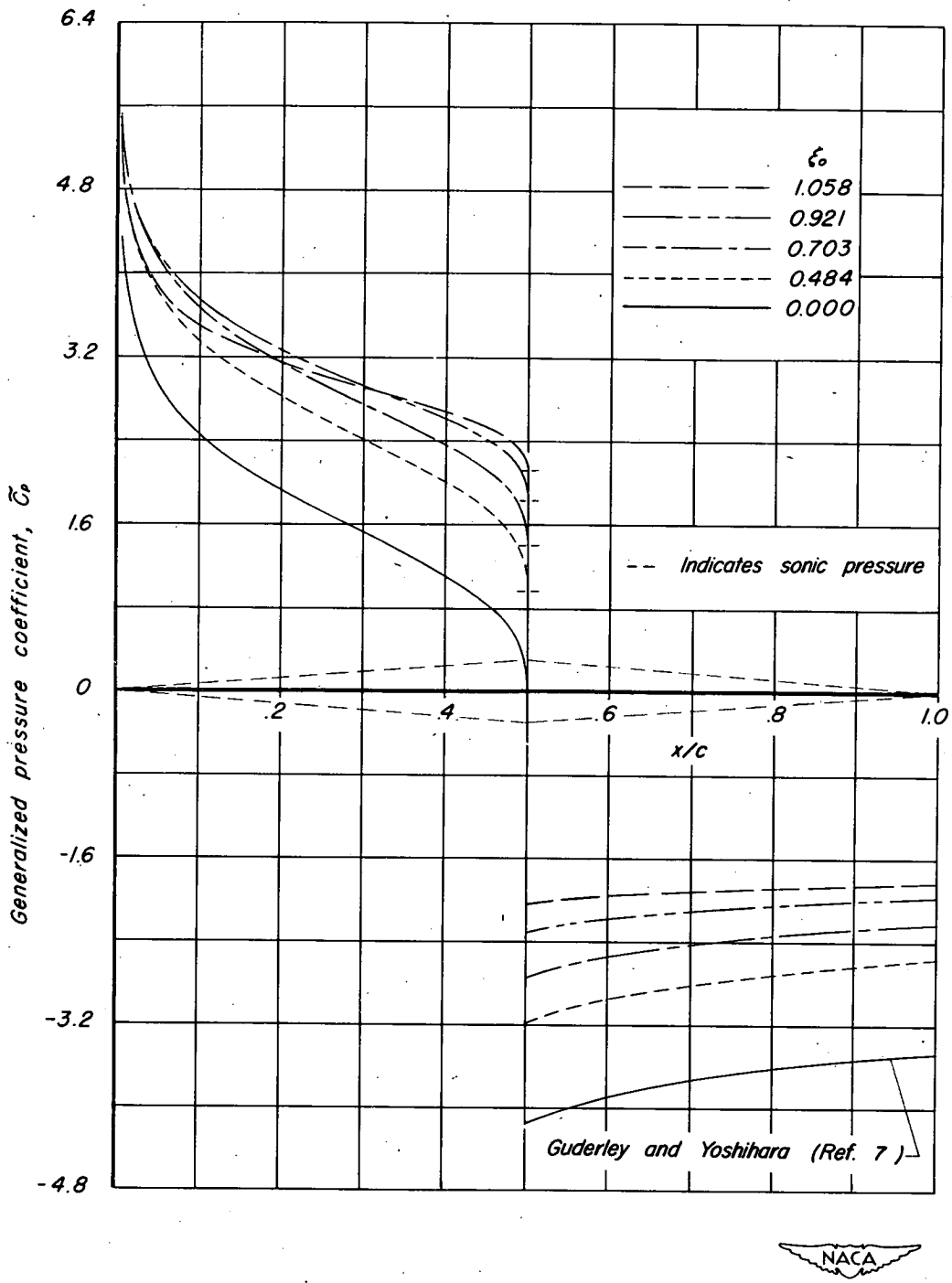

Figure 5.– Chordwise distribution of generalized pressure coefficient at surface of airfoil.

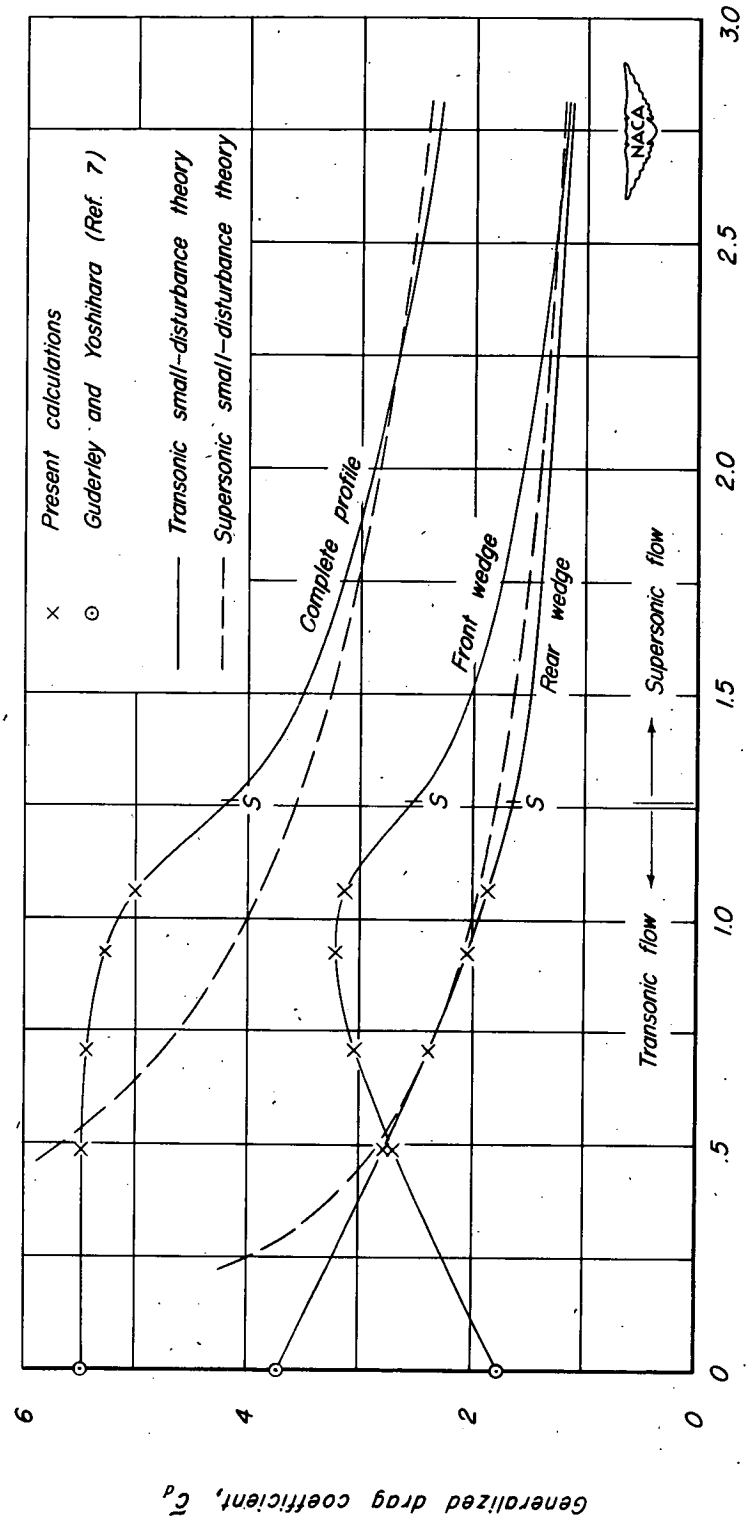

Figure 6.- Variation of generalized drag coefficient.

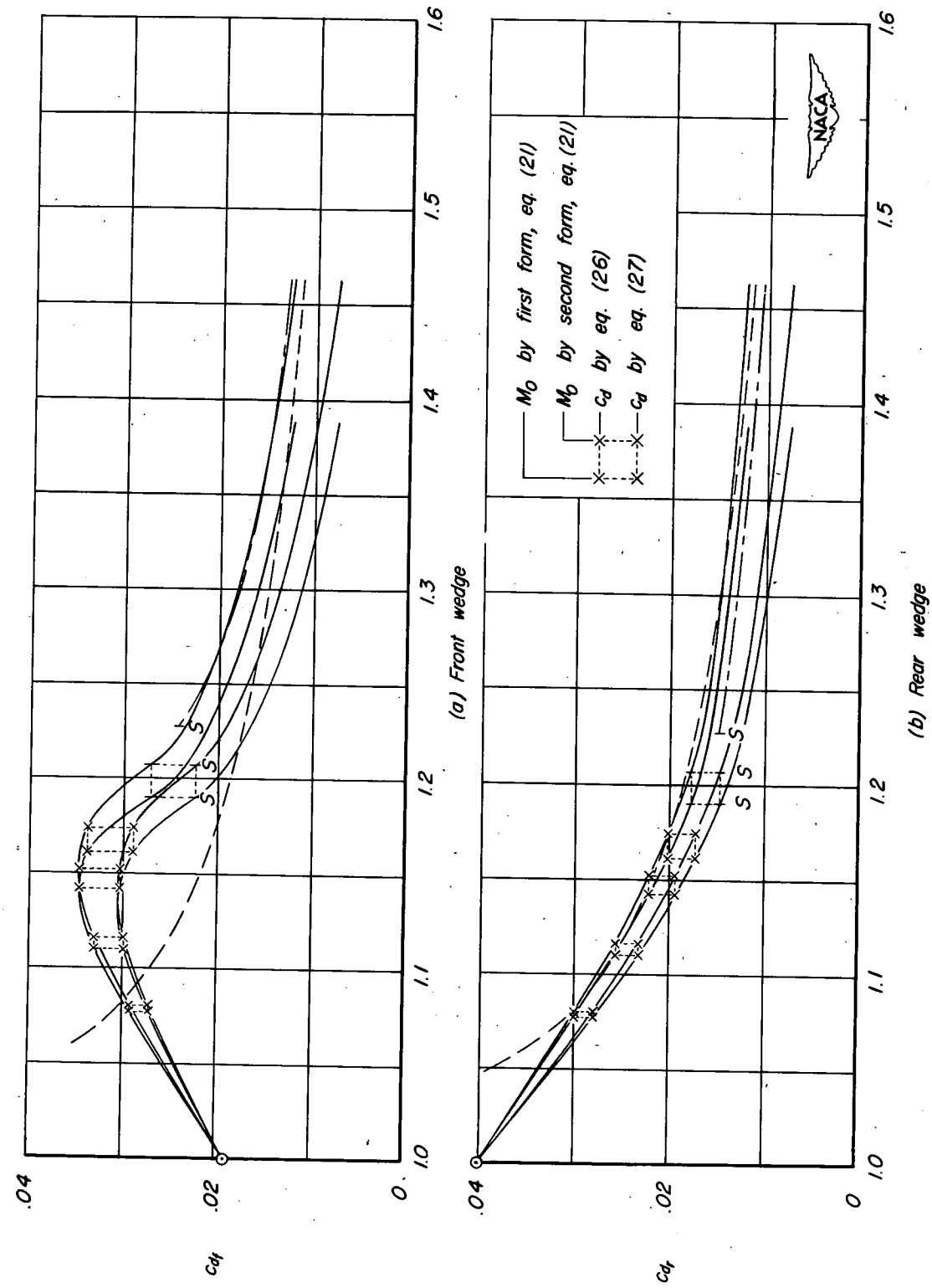
M_0 by first form, eq. (21)
M_0 by second form, eq. (21)
c_d by eq. (26)
c_d by eq. (27)
NACA
.04
.02
0
c_{df}
1.0
1.1
1.2
1.3
1.4
1.5
1.6
S
(a) Front wedge
(b) Rear wedge

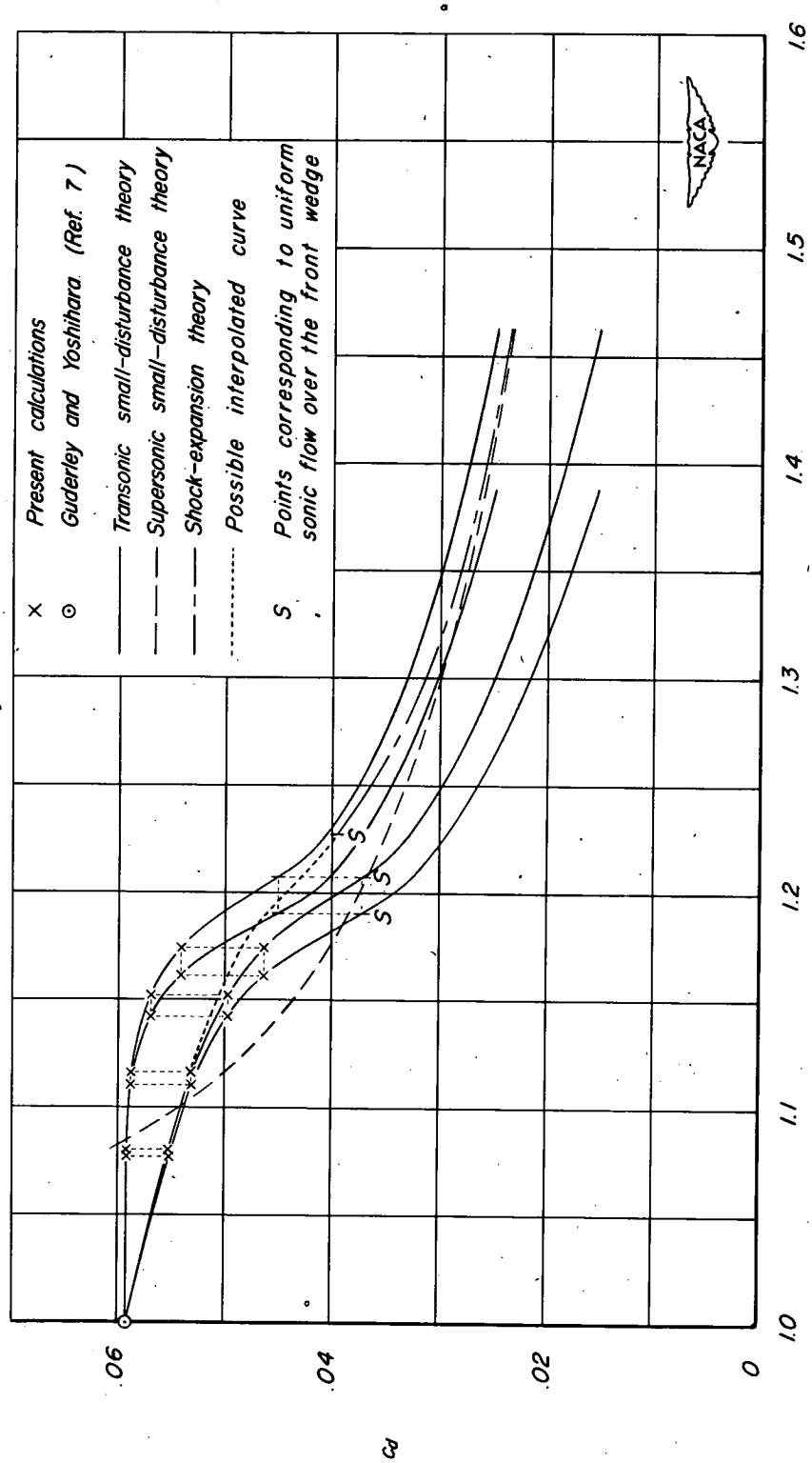

(c) Complete profile

Figure 7.— Variation of drag coefficient with Mach number for t/c = 0.0787 and $\gamma = 1.4$.